CHARLES UNIVERSITY IN PRAGUE

FACULTY OF SCIENCE

Department of Experimental Plant Biology

In planta production of TMV (tobacco mosaic virus) nanoparticles of specific length

In planta produkce nanočástic specifické délky s použitím RNA a obalového proteinu Viru tabákové mozaiky (TMV)

MASTER THESIS

Lucie Dlabalová

Supervisor: Mgr. Tomáš Moravec, Ph.D.

Prague 2013

This work was created in the Laboratory of Virology at the Institute of Experimental Botany, the Academy of Sciences of the Czech Republic, in Prague.

Prohlášení

Prohlašuji, že jsem závěrečnou práci zpracovala samostatně a že jsem uvedla všechny použité informační zdroje a literaturu. Tato práce ani její podstatná část nebyla předložena k získání jiného nebo stejného akademického titulu.

V Praze 15.8.2013 ……..

Poděkování

Zde bych chtěla na prvním místě poděkovat svému školiteli Mgr. Tomáši Moravcovi, Ph.D. za nekonečnou trpělivost a vždy přítomný optimismus, neustálý příval nových nápadů, cenné rady, přátelský přístup a spoustu času, který mi věnoval v laboratoři i při korekturách textu. Dále bych chtěla poděkovat Doc. RNDr. Noemi Čeřovské, CSc. a Dr.rer.nat. Ing. Heleně Plchové za občasné konzultace a „pevnou ruku“ a všem z našeho laboratorního týmu, tedy Renatě Hadámkové, Dáše Cibochové a Petrovi Vaculíkovi, za metodologickou pomoc a uvedení do laboratorního světa.

Děkuji své mamince Naděnce a Standovi za to, že mě podporují, abych mohla dělat to, co je mi nejbližší a co mě baví a za to, že jsou. Můj dík patří i Adélce Šímové a Mirkovi Tichému za korektury v textu a všem přátelům, s kterými jsem se mohla příležitostně rozptýlit ve stínu lapiny (*Pterocarya*). Na neposledním místě chci zmínit svého skvělého přítele Martina, který se stal (ne)dobrovolně prvním čtenářem a kritikem celé práce, vždy mi s čímkoliv pomohl, ať už se jednalo o technickou či jazykovou stránku věci, a který mi vyjde vždy vstříc a je mi velkou oporou.

Abstract

Tobacco mosaic virus (TMV) is one of the most investigated viruses and its attributes and structure are therefore well-known. In this work, we have chosen TMV as a biotemplate for the adjustable-length particles production in plants. The viral RNA and coat protein of TMV self-assemble into particles under physiological conditions. The particle length depends on the length of packaged RNA. The encapsidation signal that is necessary for preferential viral RNA packaging by coat protein disks is known and characterized since the 1980´s.

In this work, we have proposed a two-component system based on a *Nicotiana bentamiana* plants infection with packaging competent defective RNA (dRNA) and a helper virus RNA which provides all the components necessary for dRNA replication and packaging. The encapsidation signal in the helper virus sequence was removed to avoid formation of particles of incorrect length. Some of our helper viruses contained a coat protein with modified region of the particle's inner channel. This modification should allow specific binding of metal atoms within the core of the rod shaped particle. Several variants of dRNA and helper viruses were prepared to identify individual areas important for the replication, encapsidation and nanoparticle stability. We focused on the particle formation ability in plants, identification of RNA contained in the particles and distribution of particle lengths in the population.

We have surprisingly discovered that the encapsidation signal elimination from the viral genome does not affect the particle assembly, only the virus sensitivity to higher temperatures. This interesting discovery had an impact on our proposed system when the helper virus particles substantially prevailed over the target-length particles. We constructed a virus with a metal-binding peptide that is exposed in the particle's inner channel. This virus retains its infectivity and the ability to create particles. The length distribution of particles, however, revealed that the specificity of such a modified coat protein for the viral RNA was impaired. The individual components of the proposed system seem to be very promising and could have broad potential use both in scientific research and in biotechnology applications. Further research will be necessary to use the dRNA vectors and modify the system components to ensure the uniform particle length. Further research might also improve our understanding of the mechanisms of viral RNA encapsidation in plants.

Key Worlds: Tobacco mosaic virus, TMV, nanoparticles, origin of assembly, encapsidation signal

Abstrakt

Virus tabákové mozaiky je jedním z vůbec nejprozkoumanějších virů, jeho vlastnosti a struktura jsou plně známy. Z tohoto důvodu byl v této práci vybrán jako biotemplát pro tvorbu nanočástice nastavitelné délky. Pokud je za fyziologických podmínek přítomna jak virová RNA, tak obalový protein, částice jsou schopny se samouspořádat a jejich délka je závislá na délce balené RNA. Podmínkou přednostního balení virové RNA je přítomnost enkapsidačního signálu, který byl identifikován již v 80. letech.

V této práci jsme vytvořili dvoukomponentový systém, kdy byly rostliny *Nicotiana bentamiana* infikovány defektní RNA (dRNA) určenou k zabalení a RNA pomocného viru poskytující všechny komponenty nutné pro replikaci a balení dRNA. V RNA pomocného viru byl navíc vyřazen enkapsidační signál, aby nedocházelo k balení nesprávně dlouhých částic. Některé námi vytvořené pomocné viry navíc obsahovaly obalový protein modifikovaný v oblasti vnitřního kanálu částice. Tato modifikace by měla v budoucnu umožnit specifické vyplnění částic kovem. V rámci práce bylo připraveno několik variant jak dRNA, tak i pomocných virů, aby bylo možné identifikovat jednotlivé oblasti důležité pro replikaci, stabilitu a enkapsidaci vznikajících nanočástic. U rostlin infikovaných jednotlivými systémy jsme poté zjišťovali hlavně to, zda došlo k tvorbě částic, jakou RNA částice obsahovaly a jaké bylo rozložení délek v populaci částic.

Zajímavým a neočekávaným zjištěním během vytváření pomocných virů bylo to, že odstraněním enkapsidačního signálu z genomu viru se prakticky nijak nezměnila schopnost tvorby částic, zvýšila se jen citlivost viru k vyšším teplotám. Tento fakt měl dopad na námi navrhovaný systém, kdy v celkové populaci vzniklých částic výrazně převažovaly úplné virové částice obsahující pomocnou RNA. Podařilo se nám vytvořit virus s kov-vázajícím peptidem exponovaným ve vnitřním kanálu částic, který si zachoval infektivitu i schopnost tvorby částic. Distribuce délky částic tohoto viru nám však napověděla, že specifita takto modifikovaného obalového proteinu k virové RNA byla narušena. Jednotlivé komponenty navrhovaného systému se jeví jako velmi slibné a s širokým potenciálem využití ve vědeckém výzkumu a v biotechnologiích. V další práci bychom se rádi věnovali využití dRNA vektorů a úpravě komponent systému tak, aby vnikaly převážně částice jedné délky. K tomu bude zapotřebí objasnit i mechanismus enkapsidace virové RNA v rostlinách.

Klíčová slova: Virus tabákové mozaiky, TMV, nanočástice, enkapsidační signál

CONTENTS

List of Abbreviations

A. tumefaciens	*Agrobacterium tumefaciens*
CaMV	Cauliflower Mosaic Virus
CP	Coat Protein
DNA	DeoxyriboNucleic Acid
dpi	days *post* infection
E. coli	*Escherichia coli*
ELISA	Enzyme-Linked Immunosorbent Assay
F	forward
GFP	Green Fluorescence Protein
Hc-Pro	Helper-component Proteinase
HR	Hypersensitive Response
kb	kilobases
MP	Movement Protein
N.	*Nicotiana*
NTR	Non-Translated Region
OAS	Origin of ASsembly
ORF	Open Reading Frame
PCR	Polymerase Chain Reaction
R	reverse
RdRp	RNA-dependent RNA polymerase
RE	Restriction Enzyme
RNA	RiboNucleic Acid
RT-PCR	Reverse Transcription PCR
sg	subgenomic
SOE-PCR	Splicing by Overhang PCR
TMV	Tobacco Mosaic Virus
VLP	Virus-Like Particles
wt	wild type

1. INTRODUCTION

1.1. Brief history of tobacco mosaic virus (TMV)

Tobacco mosaic disease was first described in 1886 by A. Meyer. In 1892 D. Iwanowski specified that the disease is caused by an unknown infectious and filterable agent for which M. Beijerinck coined the term "virus" (Beijerinck, 1889). So the tobacco mosaic virus became the first virus to be discovered.

First crystallization of the virus was performed on TMV by W. M. Stanley in 1935. Due to the new consequences determined from the fact that the isolated crystals remained infectious Stanley won the Nobel Prize in 1946. In 1939, TMV was the first virus visualized by electron microscopy. TMV´s coat protein became the first viral protein whose primary structure was deciphered in 1960 and many mutants of this protein helped to confirm its genetic code. In 1982, the TMV was the first plant virus whose genome was sequenced, and the structure and function of genes became known (Goelet et al., 1982). TMV has contributed to the development of molecular biology, virology, biochemistry and biotechnology for its simplicity, stability, and high titre in host plant tissues.

1.2. TMV: biology and structure

Tobacco mosaic virus is a member of the genus *Tobamovirus* and is classified in family *Virgaviridae*. Tobamoviruses are divided into many strains. The most widespread and investigated strain is the TMV-U1 (syn. *vulgare*) – which was used as a model also in this work. The second most studied TMV strain is the TMV-L (tomato mosaic virus or ToMV; Ohno et al., 1984).

TMV virions are rod-shaped hollow particles having about 300 nm in length, 18 nm in width and the internal channel with a diameter of 4 nm. Genomic RNA is twisted into the helix at a radius of 6 nm (Namba et al., 1989). RNA is protected by a capsid that consists of 2130 molecules of coat protein (CP). There are 16 $\frac{1}{3}$ CP per helix turn and one monomer of CP binds to three adjacent RNA nucleotides. Thus the virion is composed of only two components, the weight ratio of which is 95: 5 (CP : RNA; summarized in Butler, 1999).

One of the known features of TMV particle is its high stability, particularly at high temperatures, upon desiccation, freezing and thawing (Rogers et al., 2004). At temperatures below 40 °C, the particles remain infectious for decades. Hydrophobic electrostatic

interactions and the formation of so-called ‘‘Caspar’’ carboxylate pairs (see 1.6) contribute to the high particle stability (Kegel & van der Schoot, 2006). The particle stability is dependent on pH, ionic strength and presence of Ca^{2+} ions. At pH values above 8, the stability significantly decreases and CP predominates in a dissociated state, the bonds between CP and RNA are disrupted. It is interesting that Tobamovirus particles have shown to maintain infectivity even after passage through the digestive system, or after prolonged retention in lungs of smokers (Balique et al., 2012; 2013).

TMV is widespread throughout the world which is also enabled by its wide host range. The virus is known to infect about 200 species from 30 plant families (Shew et al., 1991). The most common host is the genus *Nicotiana* and plants of the family *Solanaceae*. There is no known insect vector, also its transmission by pollen or seeds has not been described. The virus is exclusively mechanically transmissible, what is facilitated by its extremely high accumulation levels in plant tissues. Symptoms are dependent on the plant species, virus isolate and its physiological conditions. The most common symptoms are mosaics, discolorations or necrotic lesions on infected leaves, distorted and chlorotic young upper leaves, and in the case of serious damage of vasculars, the plant can dry out and die. The way to diagnose the TMV with certainty is the ELISA or RT-PCR because there is high variability in TMV symptoms.

One of the options for the protection of plants against viruses is the cross-protection. Here the plant is infected with less virulent or attenuated strain of the virus, making it resistant to highly virulent strain as summarized in Gonsalves et al. (1989). Alternative strategy relies on the use of transgenic plant with transferred part/(-s) of the viral genome (Abel et al., 1986). This situation evokes so called “pathogen-derived resistance” in the plant. The protection mechanism in this case is the gene silencing (Baulcombe, 1996).

1.3. TMV: genome organisation

Genome of TMV consists of a positive single-stranded RNA which has 6395 nucleotides in length. There is a methylguanosine cap ($m^7G^{5'}ppp^{5'}Gp$) situated at the 5′end. Compared to the eukaryotic cap, the first two bases behind the cap are not methylated (Zimmern, 1975). RNA itself is infectious due to the positive-sense coding, however, its infectivity is largely lost upon removal of the cap (Ohno et al., 1976). The cap is connected to 68 bases of non-coding AU-rich sequence (non-translated region, 5'NTR), also known as the omega enhancer (Ω leader; Richards et al., 1978). It is known that this sequence is able to enhance

translation of foreign genes, which has been widely used in genetic engineering of transgenic plants and other organisms (Rosypal, 2006). Genomic RNA is terminated by another NTR (3'NTR) which is 204 bases long and ends with dephosphorylated adenosine (Guilley et al., 1979). The 3'NTR may be folded into a secondary structure which forms tRNA-like terminus of three consecutive pseudoknots (Rietveld et al., 1984). It is possible to *in vitro* aminoacylate this terminus by histidine (Öberg & Philipson, 1972). Thus the secondary structure of the 3'end of viral RNA perfectly mimics the polyA of mRNAs in plant and animal cells (Gallie & Walbot, 1990). Removal of 3´NTR results in loss of infectivity of the virus (Takamatsu et al., 1990) due to the subsequent recognition and degradation by cellular mechanisms.

The genome contains four open reading frames (ORF), the products of which are three non-structural proteins and one structural protein. The first ORF starts downstream of the Ω enhancer and the product is a 126 kDa protein with a leaky termination codon. The read-through of this codon is translated to 183 kDa protein in approximately 2 to 5% of all transcriptions. Products of the last two ORFs are 30 kDa movement protein (MP) and 17.5 kDa coat protein (CP) which are translated from two individual subgenomic RNAs (sgRNA). Only the ORF closer to the 5´end is translated from these subgenomic RNAs. This mechanism guarantees translation enhancement and is used by many other viruses, however, it was first observed in TMV. While 5'NTR region contains sequences necessary for the translation initiation, 3'NTR region contains *cis*-acting sequences required for replication. Viral RNA thus contains *cis*-acting sequences for translation, sgRNA synthesis, replication and virion assembly (summarized in Goelet et al., 1982 and Okada, 1999).

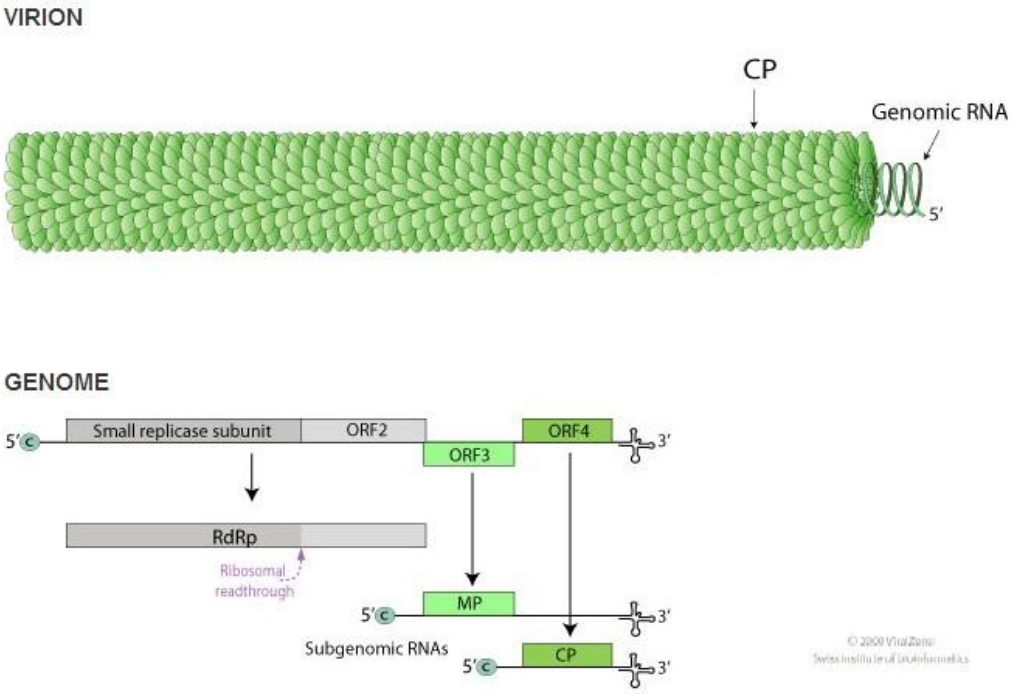

Figure 1: TMV structure and genome. Adapted from viralzone.expasy.org.

1.4. Virus-encoded proteins

1.4.1. Replicases

Protein products of ORF1 and ORF2, which is translated after read-through of "leaky" stop codon at the end of ORF1, are replicases with a molecular weight of 126 kDa and 183 kDa. Both proteins contain N-terminal domain with methyltransferase and guanylyltransferase activities (Dunigan & Zaitlin, 1990) and helicase domain (Goregaoker & Culver, 2003). The read-through domain, which is contained only in a 183 kDa protein contains motifs characteristic for RNA-dependent RNA polymerase (RdRp; Kamer & Argos, 1984). RNA 5´NTR and 3´NTR regions serve as *cis*-acting sequences for replicase binding. Sequences in replicases were identified that are required for binding of movement protein and cell-to-cell virus spread (Knapp et al., 2007). Isolated replication complex was found to contain not only the 126 kDa and 183kDa proteins, but also the host 56 kDa protein, which corresponds to the RNA-binding subunit of yeast translation initiation factor eIF-3 (Osman & Buck, 1997).

The 183 kDa protein is essential for replication and sgRNA transcription. The deletion mutant without ORF3 and/or ORF4 is able to replicate in infected cells implying also that there are no *cis*-acting sequences affecting replication in this part of the genome (Meshi et al., 1987). Furthermore, the mutant without 183kDa protein is not infectious and mutant producing only

183 kDa protein, without 126 kDa protein, has a reduced infection ability (Ishikawa et al., 1986). Mutations in both replication proteins of tobamoviruses may lead to the host specificity alteration (Hamamoto et al., 1997).

The helicase domain is also the symptom determinant of the hypersensitivity response (HR; Les Erickson et al., 1999). Based on the HR, F. O. Holmes developed the necrotic local lesion assay method in 1929 which is used to determine the number of infectious virus particles in the plant extract by generated lesions. This biological test can be applied only to plants with *N* gene as *Nicotiana glutinosa*, *N. tabacum* cvs. Xanti-nc or *N.t.* Samsun NN. Almost all tobamoviruses cause HR in appropriate plant hosts, but certain strains are capable of overcoming this resistance (Padgett & Beachy, 1993).

1.4.2. Movement Protein (MP)

The ORF3 encodes the 30 kDa movement protein which is involved in virus spread through plasmodesmata to adjacent cells (Kawakami et al., 2004). MP is able to expand the original 3 nm plasmodesmata size to 6 nm and thus physically facilitate movement. The C-terminal protein domain has the ability to bind plasmodesmata while the N-terminal domain is typically bound to a single-stranded nucleic acid (Citovsky et al., 1990). The interactions between MP and cytoskeletal microtubules have been observed, apparently on the way to or from plasmodesmata (McLean et al., 1995).

Movement protein of TMV was the first described viral protein required for the virus spread (Deom et al., 1987). Subsequently, similar proteins have been found in many other plant viruses. Some viruses, including tobamoviruses, can facilitate other viruses to spread in a particular plant host when the second virus is incompetent of its independent spread. This suggests that the interactions between viral proteins and host factors are more precise than those with viral RNA. The overall virus ability to spread through the plant is however determined by further interactions between the plant and the virus (Fedorkin et al., 1997).

1.4.3. Coat Protein (CP)

ORF4 encodes the coat protein with 17.5 kDa molecular weight. The main function of CP is to bind and intercalate the genomic RNA between protein disks and thereby protect RNA against cellular nucleases and environmental factors. Monomer CP consists of 159 amino acids that are folded into four α-helices connected by loops (see Figure 2). The protein regions exposed on the surface of the virion are N-terminus, C-terminus and the surface loop of amino acids 55 - 60, while amino acids 94 - 106 are exposed to the inner channel of particle (Lu et al., 1998). Under physiological conditions, the CP monomers have the ability to polymerize into short virus-like particles (VLP) without the viral RNA presence (summarized in McCormick & Palmer, 2008) .

Besides its structural role, the CP is also necessary for virus long-distance movement through the phloem to the uninfected upper-leaves (Dawson et al., 1988). Therefore the formation of viral particles is essential for virus spread through the whole plant. CP is further considered to be the symptom determinant affecting the host symptoms and elicitor of plant defence mechanisms in some sensitive hosts such as *N. sylvestris*. In this case, the alteration of CP may lead to the hypersensitivity response after interaction with host *N´*gene product (Knorr & Dawson, 1988).

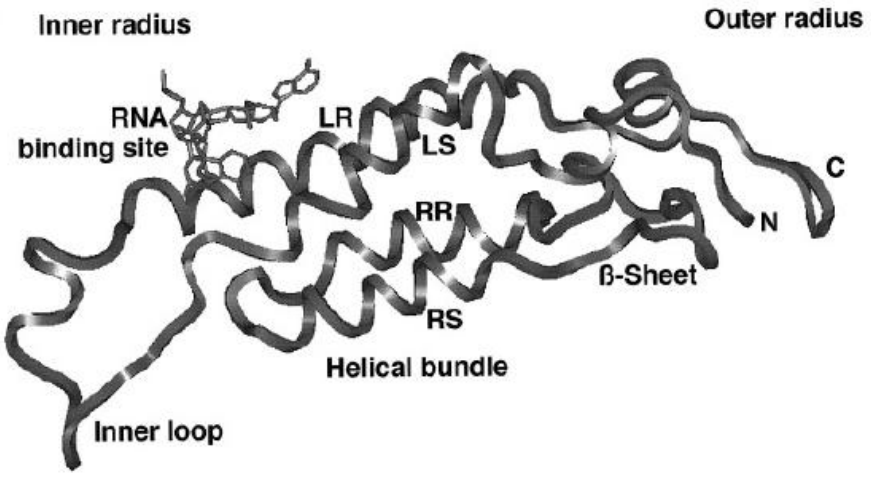

Figure 2: Single coat protein subunit structure. The four α-helices are labelled LS (left slewed), RS (right slewed), LR (left radial), and RR (right radial). The inner loop connects the LR and RR helices. The RNA-binding site is formed by residues from both loops and the LR helix. The N- and C-terminal are at the outer radius of the virus. Adapted from Lu et al. (1998).

1.5. Replication cycle

The RNA release from the capsid is needed after virus penetration into the cell. Virion disassembly is driven by repulsion of negatively charged carboxylate groups of amino acids aspartate and glutamate (Caspar, 1964). The TMV structure forces the carboxyle groups of neighbouring CP subunits to close proximity and create so called “Caspar” carboxyl-carboxylate pairs binding proton or calcium ions with high affinity. After penetration, the high pH and low calcium concentration of plant cell cytosol, in contrary with extracellular pH, remove proton and calcium ions from the carboxyl-carboxylate and carboxyl-phosphate pairs. This results in repulsion between carboxylates and it destabilizes the virion structure at the 5´end and forces the 20S protein subunit disassembly (Wang et al., 1998). Only then the RNA 5´NTR associates with the host ribosome. Ribosome binding initiates another dissociation of CP monomers so the ORF1 and ORF2 can be translated while the particle is unpackaged; this process is called "co-translational disassembly" (Wilson, 1984). At the beginning, the particle disassembly is very fast and in the first three minutes after inoculation there is usually released around 4635 nucleotides at the 5'end, which corresponds to ORF2 (Wu et al., 1994). Several antibodies inhibiting TMV dissasembly and spherically preventing RNA and ribosome interaction were found. Such antibodies expressed in plants could prevent virus infection (summarized in Okada, 1999).

The translation of replicase proteins is crucial for the initiation of replication cycle. Subsequently, replicase synthesizes the negative strand according to the positive genomic RNA strand. The resulting dsRNA serves as a template for replication / transcription of genomic RNA and both sgRNAs. The negative RNA strand synthesis is stopped shortly after infection, whereas the synthesis of positive RNA strand continues to be encapsidated into the particles in the late stage of the cycle. During the late phase of the cycle the CP accumulation occurs, resulting in the beginning of highly organized process of spontaneous particle assembly.

As already mentioned above, the MP and CP translation is realized from its own sgRNAs. MP is produced in early phase of the infectious cycle and accumulates in low level, while the CP is persistently produced later and accumulates in high levels (Watanabe et al., 1984). This timing and quantity distribution of translation is given by the subgenomic promoter sequences (Lehto et al., 1990), which are located upstream the sgRNA ORFs. Compared to the MP promoter, the CP promoter requires for its full activity even the sequences within

ORF4. The strength of CP promoter is very useful in expression systems based on tobamoviruses. Foreign sequences inserted behind the tobamoviruses promoter were expressed at high levels in plants (summarized in Gleba et al., 2007).

At the beginning of infection cycle the virus spreads from infected to adjacent cells through plasmodesmata as intact replication complexes (Kawakami et al., 2004). Once the first complete virions are assembled, the virus is able to penetrate into the phloem. This is followed by rapid long-distance movement to the young non-infected upper-leaves and other plant organs. When the particle formation is blocked, virus cannot spread through whole plant and does not cause typical mosaic symptoms. The replication maximum in infected cells is achieved between 16 – 96 hours after infection, then it stops. Replication and virion assembly takes place in the cytoplasm at the so-called "replication factories". Viral RNA is associated with perinuclear endoplasmatic reticulum in the early stage of infection then the virions disperse throughout whole cytoplasm by microtubules (Más & Beachy, 1999). Cells remain metabolically active for a long time, although the apparatus is controlled by a virus (summarized in Okada, 1999).

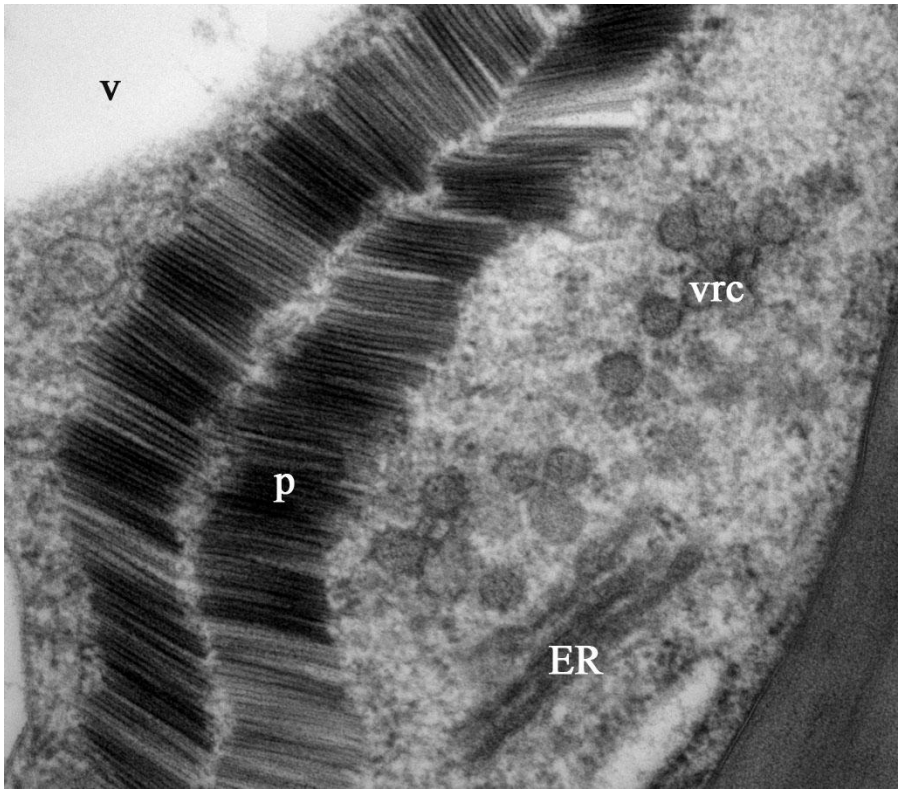

Figure 3: Cytoplasm of tobacco cell infected with TMV-U1. (v) vacuole, (p) virus particles, (vrc) Endoplasmatic reticulum-derived replication complexes, (ER) Endoplasmatic reticulum. Transmission electron microscopy picture obtained by high-pressure freezing method, from Moravec.

1.6. Virion assembly

In 1955, H. Fraenkel-Conrat and R. Williams performed *in vitro* experiments proving that infectious particles are able to self-assemble from isolated RNA and CP subunits under physiological conditions. The CP subunits can aggregate to small heterogeneous aggregates of various lengths even without RNA on the base of protein-protein interactions (Fraenkel-Conrat & Williams, 1955). However, this process is dependent on the pH and ionic strength. The most common is the 20S aggregate (20S correspondents to the sedimentation coefficient), a two-layer cylindrical structure in disk form. Each layer consists of circle of 17 CP subunits compared to 16 $\frac{1}{3}$ CPs per helix turn in virion structure. Under suitable conditions, the connection of disks occurs. The longer polar or non-polar protein helixes are formed and the polarity depends on the orientation of adjacent discs (summarized in Klug, 1999).

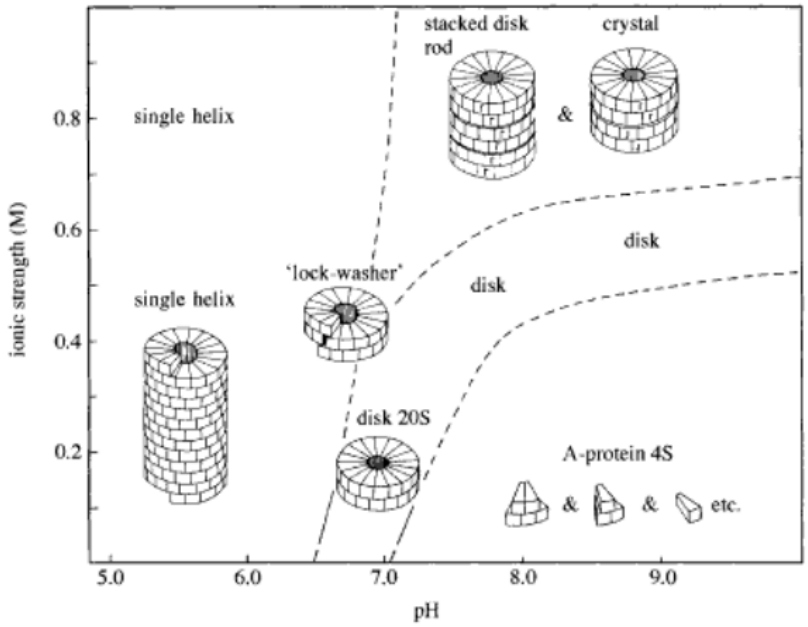

Figure 4: Diagram of TMV CP aggregates under variable conditions (pH and ionic strength). The single helix represents aggregate formed after several disks connection. The "lock-washer" is an unstable form at the interface between 20S disk aggregate and the helix. The 20S aggregate is the dominant form at pH 7 and 0.1 molarity. At higher pH the disks disintegrate to smaller A-protein 4S aggregates. The aggregate forms are approximately correct for a protein concentration of 5 mg / ml at 20 °C. Adapted from Klug (1999).

Protein disk of 20S aggregate plays a crucial role in particle assembly initiation (Butler & Klug, 1971). 20S aggregate is recognized by specific sequence of origin of assembly (OAS) which is located about 1000 nucleotides upstream RNA 3´end. The harpin structure of the OAS is inserted through the central hole of 20S aggregate with both RNA ends protruding

from one side. During the bidirectional particle elongation, the RNA is pulled through the inner channel and the 20S aggregates constantly bind to forming RNA loop towards particle 5´end while the RNA 3´end is retained on the other side of particle. The particle elongation towards the 5´end is faster in contrast with the growing towards the 3´end where the smaller A-protein 4S aggregates bind (summarized in Butler, 1999).

The TMV-U1 OAS sequence is located in MP ORF at 5420 – 5546 position in TMV genome and its secondary structure forms three stable hairpin loops (Zimmern & Butler, 1977). *In vitro* experiments in the 80´s identified putative OAS core consisting of 75 bases long tract (OAS_{75}). OAS_{75} forms stem-loop structure (loop 1, the 3´end most) with the crucial sequence AAGAAGUCG exposed as a single strand on its apex which is sufficient to direct encapsidation of heterologous RNA fragments by TMV CP. Alteration or deletion of this sequence, or the loop shortening, leads to the abolishing of the rapid packaging which is then apparently sequence non-specific. The three-base G periodicity within this sequence element is an important feature in assembly nucleation (Turner & Butler, 1986; Turner et al., 1988).

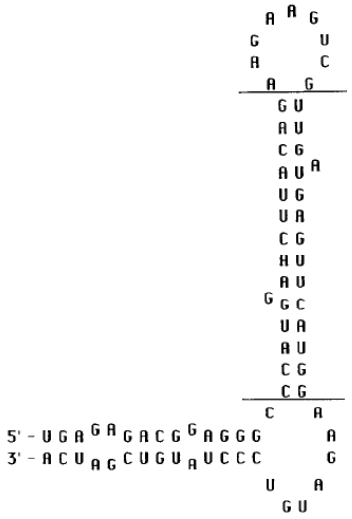

Figure 5: The TMV-U1 origin of assembly RNA hairpin loop 1 adapted from Turner et al. (1988)**.** The sequence and structural analysis by Zimmern & Butler (1977) amended with point mutations found in later Cambridge preparations (Goelet et al., 1982) to give the apex sequence AAGAAGUCG.

OAS is responsible for preferable viral RNA packaging, but a small amount of non-viral RNA was also found in naturally encapsidated particles (Siegel, 1971; Rochon & Siegel, 1984). The OAS sequence integration into foreign RNA with TMV CP co-expression can be used to foreign RNA trans-encapsidation (Sleat et al., 1988). In addition to full-length virus rods in the isolated TMV particles, a heterogeneous population of shorter rods is presented due to the sgRNAs expression where the OAS sequence is contained (Beachy & Zaitlin, 1977).

1.7. TMV and biotechnology

TMV seems to be very promising tool for biotechnological applications and offers many advantages. It has a simple and well-known structure of virion and CP which allows easy design of modifications both on the surface and inside the particle. Particles can be decorated with suitable ligands (for example antibodies, peptides or metals) to create highly immunogenic carriers (summarized in Smith et al., 2006). Rod-shaped particles enter into animal cells more efficiently than the spherical particles (Shukla et al., 2012) and particles derived from plant viruses are considered to be safer for human medicine than animal viruses (Destito et al., 2009). Plant viruses are generally more stable compared to the animal viruses for example in the gastrointestinal tract (Rae et al., 2005). TMV has the ability to self-assembly and for some applications the rod shape is preferable. TMV is able to replicate in plants to high titres and its purification is relatively easy (advantages summarized in McCormick & Palmer, 2008). TMV particles are also frequently used as a gene vectors carrying foreign sequences.

A large part of the CP polypeptide chain is antigenic which makes the TMV a very good immunogen. In a recent study (Liu et al., 2013) TMV antibodies were found even in humans. The effect on health is still under investigation. Viral particle and dissociated CP carry different epitopes due to their quaternary structure and thus they can be targeted by different antibodies. For the CP modification and peptide insertion, N- and C-terminus, surface loop (amino acid residues 59 – 65) and inner channel loop is suitable (Turpen et al., 1995). The inserted peptide should however not be longer than 20 - 25 amino acids in order to avoid spherical problems and particle instability (McCormick & Palmer, 2008). One of the possible ways to overcome this limitation is flexible linker insertion between the CP and the recombinant peptide/protein (Werner et al., 2006). Another alternative method is a point mutation at the virion surface adding reactive amino acids lysine or cysteine. These amino acids then allow easy *in vitro* chemical binding of peptide or protein to the particle after its isolation from plants (Yi et al., 2005).

TMV particles may not serve only as highly immunogenic carriers. After their modifications, these particles may bind various metals by reduction reactions and create magnetic nanoparticles (Dujardin et al., 2003; Lim et al., 2010). Magnetic nanoparticles are being recently studied with much interest from diverse fields such as nanotechnology, medicine, environmental remediation or electronics. Technologies based on magnetic nanoparticles are

routinely applied to biological systems for diagnostic or therapeutic purposes (magnetic resonance imaging or magnetic fluid hyperthermia; Manchester & Singh, 2006). The properties of these particles vary depending on their shape and size. There are several disadvantages of plain metal magnetic particles of nano-sizes. They tend to aggregate and they also substantially react with each other due to their large surface. Then the nanoparticles coated with any organic polymer (such as virus capsid) are more suitable, especially for biomedical applications. Great attention has been recently given to so-called "smart" nanoparticles. Their surface is provided with ligands directing particle towards the specific destination in the patient´s body. This allows delivery of a minimal dose of drug to the target tissue. Such application of nanoparticles might be very useful for more efficient cancer therapy (summarized in Lu et al., 2007).

Many studies have focused on the TMV particles surface metallization, but the modification of inner channel of TMV for metal materials binding is still a relatively unexplored area. The fact that in this limited space the metal nanoparticle can be formed was demonstrated when the wild type TMV-U1 particles were used for the copper or silver nanoparticles production (Balci et al., 2006; Dujardin et al., 2003). In the work from Kobayashi et al. (2010), authors successfully modified coat protein peptide sequence in the inner channel area in order to increase the number of positive charges suitable for Co-Pt metallization.

2. GOALS

Main goals of the thesis were following:

1. Design a satellite RNA capable of parallel replication in dependence on TMV RNA.
2. Prepare DNA constructs containing this satellite RNA (dRNA) as short as possible with the encapsidation signal and a suitable reporter sequence. The main characteristic of dRNA should be the interaction with TMV coat protein and assembly to particles. Additional feature would be the ability to easily replace reporter sequence.
3. Remove encapsidation signal from TMV sequence in order to prevent packaging of genomic RNA.
4. Modify the coat protein in such a way that the inner channel attributes would be changed while the ability to bind RNA would be maintained.
5. Find out *in planta* system for the production of defined length particles containing defined RNA with modified inner channel.

3. MATERIALS AND METHODS

3.1. General laboratory and other equipment used

Autoclave PS 20A	Chirana, Czech Republic
Centrifuge Biofuge Pico	Heraeus, Germany
Centrifuge Multifuge 3S-R	Heraeus, Germany
Deep freezer Hera freeze	Heraeus, Germany
Documentation system Gel Doc EQ	BIO-RAD, USA
FEI Morgagni 268D Transmission Electron Microscope	FEI Company, USA
Homogenizer FastPrep-24	M.P. Biomedicals, USA
Horizontal Electrophoresis Apparatus Mini-Sub Cell GT	BIO-RAD, USA
Hybridiser HB-1D Incubator	Techne, Great Britain
Ice maker	Brema Ice Makers, Italy
Incubator Heraeus Function Line	Heraeus, Germany
Laboratory centrifuge Sigma 3K30	Sigma, Germany
Magnetic stirrer MM2A	Laboratorní přístroje Praha, CR
Mini Wide Vertical Gel Electrophoresis Apparatus	MS Major Science, USA
NanoDrop 1000 Spectrophotometer	Thermo Fisher Scientific, USA
PCR thermal cycler iCycler Thermal Cycler	BIO-RAD, USA
Scales Denver XE-310	Denver Instrument, USA
Spectrophotometer HEλIOS γ	Thermo Fisher Scientific, USA
Thermo block TB1	ThermoBlock Biometra, Germany
Ultracentrifuge Beckman L7-55	Beckman Coulter, USA
Universal Shaking Incubator NB-205	N-BIOTEK, Korea
Voltage source Power Pac Universal	BIO-RAD, USA
Vortex machine TOP-MIX 94323	BioBlock Scientific, Heidolph
Water purification machine Smart2Pure	TKA, Germany
Western blot apparatus OMNI-TRANS	Omni-Bio Brno, Czech Republic
SANYO growing box	SANYO Electrics, Japan

3.2. Material

3.2.1. Chemicals

Acetic acid (CH_3COOH)	Lach-Ner, Czech Republic
Acetosyringone	Serva, Germany
Acrylamide / Bis (40%)	BIO-RAD, USA
Agarose SeaKem	Cambrex, USA
Ammonium molybdate	Lachema, Czech Republic
Ammonium persulfate (APS)	Sigma-Aldrich, USA
Ascorbic acid	Penta, Czech Republic
Bacto-agar	BD, USA
BCIP/NBT	Sigma-Aldrich, USA
Bromphenol blue	Fluka, Switzerland
Carbenicillin	Duchefa, Netherlands
Chloroform	Chemapol, Czech Republic
D-(+)-trehalose dehydrate	Sigma-Aldrich, USA
Disodium phosphate dodecahydrate ($Na_2HPO_4.12\ H_2O$)	Lach-Ner, CR
dNTP mix	Thermo Scientific, USA
EDTA (Ethylenediaminetetraacetic acid)	Lachema, Czech Republic
Ethanol (EtOH)	Penta, Czech Republic
Ethidium bromide (EtBr)	Sigma-Aldrich, USA
Formvar	BDH Chemicals LtD, GB
Glycerol	Lach-Ner, Czech Republic
Glycin	Serva, Germany
Hydrochloric acid (HCl)	Spolchemie, Czech Republic
Isopropanol	Lach-Ner, Czech Republic
Kanamycin	Serva, Germany
KCl (Potassium chloride)	Lachema, Czech Republic
KH_2PO_4 (Monopotassium phosphate)	Lachema, Czech Republic
Low melting agarose SeaKem	Cambrex, USA
Mercaptoethanol	Fluka, Switzerland
MES (2-(*N*-morpholino)ethanesulfonic acid)	Sigma-Aldrich, USA
Monosodium phosphate dihydrate ($NaH_2PO_4\ .\ 2\ H_2O$)	Lach-Ner, Czech Republic
PEG 6000	Fluka, Switzerland

Peptone	Amresco, USA
Ponceau S	Sigma-Aldrich, USA
SimplyBlue SafeStain (Coomasie G-250)	Invitrogen, USA
Sodium acetate (CH_3COONA, NaOAc)	Chemapol, Czech Republic
Sodium azide (NaN_3)	Sigma-Aldrich, USA
Sodium chloride (NaCl)	Lachema, Czech Republic
Sodium dodecyl sulphate (SDS)	Sigma-Aldrich, USA
Sucrose	Lach-Ner, Czech Republic
Sulfosalicylic acid	Serva, Germany
TEMED (Tetramethylethylenediamine)	Roth, Germany
Trichloracetic acid ($C_2HCl_3O_2$)	Sigma-Aldrich, USA
Tris	Duchefa, Netherlands
Tween 20	Fluka, Switzerland
Yeast extract bacteriological	Amresco, USA

3.2.2. Commercial kits for molecular biology

- DNA isolation: QIAprep Spin Miniprep Kit (Qiagen, Germany)
- In-Fusion cloning: In-Fusion Advantage PCR Cloning Kit (Clontech, USA)
- PCR product purification, DNA fragment isolation from agarose gel and removal of some restriction enzymes from restriction reaction: High Pure PCR Product Purification Kit (Roche, Germany)
- RNA isolation: RNAzol RT Kit (MRC Molecular Research Center, USA)

3.2.3. Enzymes

- DreamTaq Polymerase + DreamTaq Buffer 10x (Thermo Scientific, USA)
- Agarase (Thermo Scientific, USA)
- M-MLV Reverse Transcriptase + M-MLV RT Buffer 10x (Promega, USA)
- RiboLock RNase Inhibitor (Thermo Scientific, USA)
- Phusion High Fidelity DNA Polymerase + Phusion Buffer 5x (New England Biolabs, USA)
- Restriction enzymes + appropriate buffers + BSA (New England Biolabs, USA)
- Shrimp Alkaline Phosphatase, SAP (Thermo Scientific, USA)
- T4 DNA Ligase + T4 DNA Ligase Buffer 10x + PEG 4000 (Thermo Scientific, USA)

3.2.4. Primers

P1 F	5′- AAAAAGCCGGCACGACACGCTTGTCTACTCC - 3′
P1 R	5′- AGTTCTTCTCCTTTACGCATGCTGTAATTGTAAATAGTAATTGT – 3′
P2 F	5′- CTATTTACAATTACAGCATGCGTAAAGGAGAAGAACTTTTCA – 3′
P2 R	5′- CATGGGCCCTCCGTCTCTCACTCGAGTTATTTGTATAGTTCATC – 3′
P3 F	5′- CTATACAAATAACTCGAGTGAGAGACGGAGGGCCCATGGAAC – 3′
P3 R	5′- ATTATGCATCTTGACTACCTGATCGACATAGGGACATCTTC – 3′
P4 F	5′- TGTCCCTATGTCGATCAGGTAGTCAAGATGCATAATAAATAAC – 3′
P4 R	5′- CTGCAGGCCAGGTTTCGTCCTC – 3′
Inf#1 F	5′- GACGGAGGGCCCATGGAACTTACAGAAGAAGTCGTT-3′
Inf#4 R	5′- AACACATCCGGGTACCTGGGCCCCTACCGGGGGTAA – 3′
TMV-3′NTR R	5′- GATTCGAACCCCTCGCTTTAT – 3′
TMV-sgCP F	5′- AAAGCATGCGATTTTGGAGGAATGAGTTT – 3′
dOAS F	5′ - GACGGAGGGCCCATGGAAAAAAGAGTGATGTCCGC – 3′
4# R	5′- TAAAGGGAACTCGAGCTGGGTACCTGGGCC – 3′
TMV-Rep3148 F	5′- CTCTGCTTTCAAGAGGGTATTCAG – 3′
dOAS2 R	5′- CCATGGTCGACATTAACAACTAGAGCCGTCTA – 3′
qCP1 F	5′- CACTACTCCATCTCAGTTCGT – 3′
qCP1 R	5′- ACCTGTACACCTTAAAGTCAC – 3′
qGFP F	5′- TTTCTGTCAGTGGAGAGGGT – 3′
qGFP R	5′- CGTGTCTTGTAGTTCCCGTC – 3′
GFP2 F	5′- TTTGCACTACTGGAAAACTACCT – 3′

3.2.5. Antibodies

- Anti-TMV primary polyclonal rabbit antibody (Agdia, USA)
- Anti-rabbit secondary goat antibody labelled by alkaline phosphatase (Sigma-Aldrich, USA)

3.2.6. Bacterial strains

These bacterial strains were used for general cloning and plasmid amplification:

- *Escherichia coli* TOP10 Cells (Invitrogen,USA)
  genotype: F– *mcr*A Δ(*mrr-hsd*RMS-*mcr*BC) Φ80*lac*ZΔM15 Δ*lac*X74 *rec*A1 *ara*D139 Δ(*ara leu*) 7697 *gal*U *gal*K*rps*L (StrR) *end*A1 *nup*G
- *Escherichia coli* Library Efficiency DH5α Competent Cells (Invitrogen, USA) genotype: F– Φ80*lac*ZΔM15 Δ(*lac*ZYA-*arg*F) U169 *rec*A1 *end*A1 *hsd*R17 (rK–, mK+) *pho*A *sup*E44 λ– *thi*-1 *gyr*A96 *rel*A1

The experimental plants were infected with:

- *Agrobacterium tumaefaciens* strain GV3101 (obtained from D. Baulcombe, John Innes Center, Norwich, Great Britain)

3.2.7. Plasmids

Vector pTZ57R/T (Thermo Scientific, USA)

Vector pTZ57R/T is suitable for direct TA cloning of PCR products with adenosine 3´end overhangs thanks to its linearized form with thymine 3´end overhangs in MCS (multiple cloning site). It carries β-lactamase gene (bla (Ap^R)) which gives the bacterium resistance to β-lactam antibiotics such as ampicillin or its more stable derivative carbenicillin. The PCR product is cloned in lacZ gene, allowing blue/white selection in suitable *E. coli* strain.

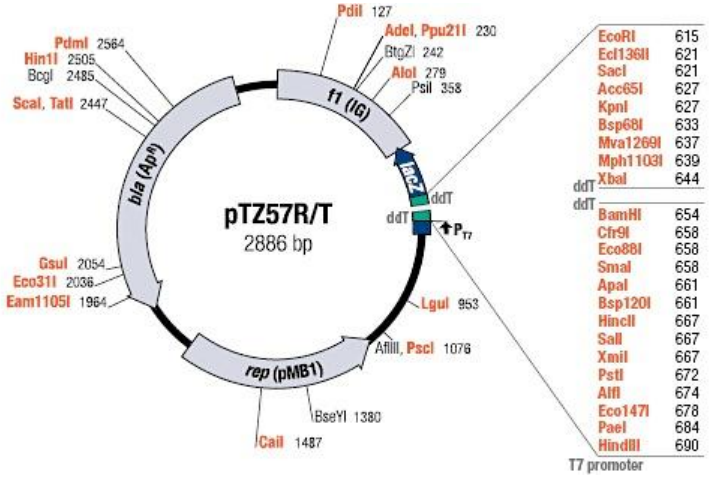

Figure 6: Plasmid pTZ57R / T: f1 (IG) – Intergenic region of phage f1, lacZ - the gene encoding β-galactosidase, rep (pMB1) - replicon of plasmid pMBI responsible for DNA replication and high number of copies, bla (Ap^R) - gene encoding the β-lactamase, PT7, T7 promoter – promoter of bacteriophage T7. Sites for restriction endonucleases are described. Adapted from www.thermoscientific.com.

Vector pGEM-T Easy (Promega, USA)

This vector has analogous properties as pTZ57R/T vector with differences in the MCS. Vectors pGEM-NAGD/CASP and pGEM-dOAS-NAGD/CASP (both provided by Mgr. Tomáš Moravec, Ph.D.) were used for cloning purposes. Both plasmids carry ORF of modified CP-NAGD/CASP but the adjacent sequences of the MP ORF differ.

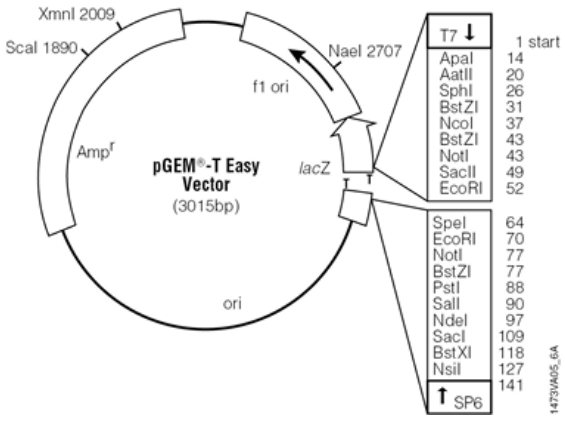

Figure 7: pGEM-T Easy vector. Adapted from www.promega.co.uk.

pGR-based vectors – provided by T. Moravec

Vector pGR is derived from the binary vector pGREEN with the ability to be maintained both in *E. coli* and in *A. tumefaciens*. Vectors by T. Moravec carry full-lentgh infectious TMV cDNA (pGR-NK2) or its modified variants. Vector contains LB and RB necessary for T-DNA integration into host genome with *A. tumefaciens* help. pGR-based vectors carry NPT I gene giving the bacteria resistance to kanamycin (Kan^R).

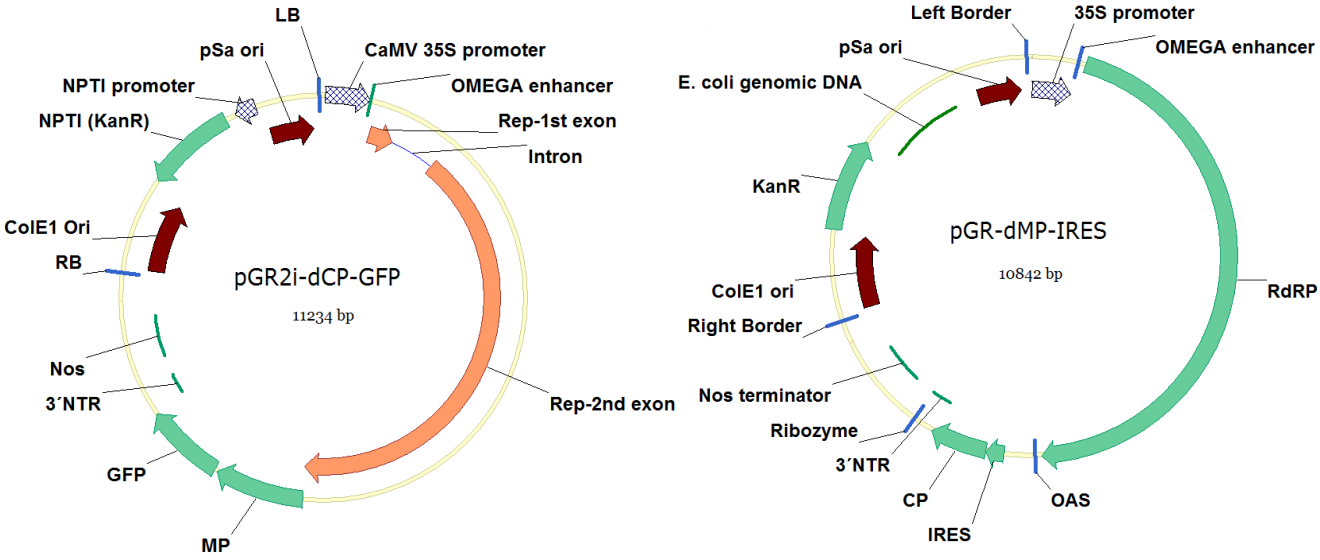

Figure 8: pGR-dCP-GFP and pGR-dMP-IRES vectors. CaMV 35S promoter – the cauliflower mosaic virus promoter, OMEGA enhancer – TMV 5´NTR, RdRp/Rep – TMV RNA dependent RNA polymerase, Intron - intron from *N. tabacum* anionic peroxidise gene, MP – TMV movement protein, GFP – green fluorescence protein, 3´NTR from TMV, Ribozyme, Nos – Nos terminator from nopaline synthetase, LB and RB - Left Border and Right Border for T-DNA transfer, ColE1 ori – vector replication origin in *E. coli*, NPTI (Kan^R) – kanamycin resistence gene (neomycine phosphotransferase I, NPT I), NPTI promoter, pSa ori - vector replication origin in *A. tumefaciens*. Figure was created in Vector NTI Advance 11 programme.

pGR2-based vectors – provided by T. Moravec

These are the second generation of infectious TMV clones with improved stability in *E. coli*. About 800 base pairs long region of the original pGR backbone with high homology to *E. coli* genomic DNA has been removed and also the orientation of the NPTI is opposite relative to the TMV cDNA, reducing the risk of TMV replicase expression in bacteria resulting from inefficient NPT I transcription termination. The starting provided vectors were pGR2i-dCP-GFP and pGR2i-TMV-dCP with CP ORF deletion.

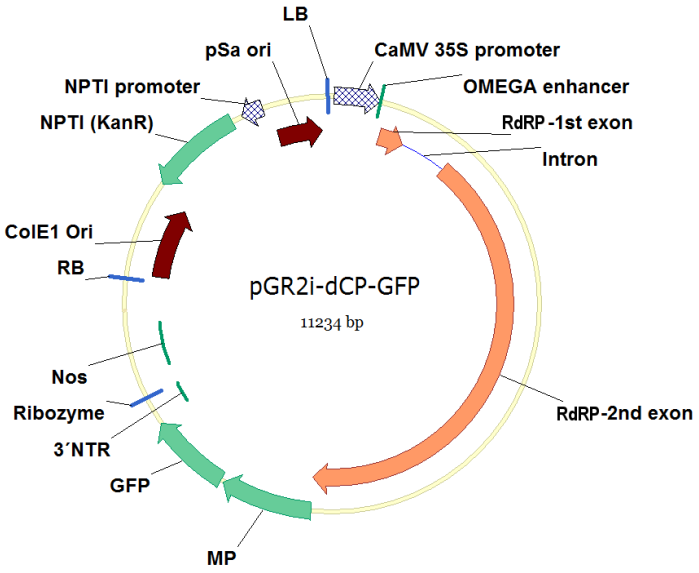

Figure 9: pGR2i-dCP-GFP vector. For more description see Figure 8.

3.2.8. Experimental plants

Non-transgenic plants:

- *Nicotiana bentamiana* (Nb)
- *Nicotiana tabacum*
- *N. tabacum*, cv. Samsun NN (Nt-NN), homozygous plants carrying *N* gene for hypersensitive response to TMV

Transgenic plants:

- Nb-MP (3H): *N. bentamiana* with TMV MP gene (provided by Dr. R. N. Beachy, Donald Danforth Plant Science Centrum, St. Louis, USA)
- Nb-MPxHCPro (K7): *N. bentamiana* homozygous plants from sexual cross of two transgenic lines, line carrying TMV MP and the second line carrying Potato Virus A Hc-Pro (suppressor of gene silencing pathway). Hc-Pro transgenic plants were provided by Dr. E. Savenkov, Department of Plant Biology, Sveriges Lantbruksuniversitet, Uppsala, Sweden.

3.3. Methods

3.3.1. Nucleic acids manipulations and cloning methods

3.3.1.1. Plasmid DNA isolation

Commercial QIAprep Spin Miniprep Kit was used for plasmid isolation from bacterial culture. The principle of QIAprep Spin Miniprep Kit is based on alkaline lysis of bacterial cells followed by adsorption of DNA on silicate fibers in the presence of solution with high ionic strength. The entire protocol was performed according to the kit instructions.

The isolated DNA concentration was then measured on NanoDrop 1000 Spectrophotometer.

3.3.1.2. Polymerase chain reaction (PCR)

PCR is used for amplification of the selected DNA segment in several repeating steps with use of thermostable DNA dependent DNA polymerase.

This method was used for the purposes of cloning and verifying the sequence presence in the sample. Two types of DNA polymerases were used. The DreamTaq Polymerase was sufficient for the sequence presence verification and TA cloning of shorter sequences (see 3.3.1.8) while the Phusion High Fidelity DNA Polymerase was used mainly for cloning of longer fragments.

The PCR reaction mix:

DreamTaq DNA Polymerase		**Phusion High Fidelity DNA Polymerase**	
Component	**Volume**	**Component**	**Volume**
10x DreamTaq Buffer + $MgCl_2$ (20 mM)	3 µl	5x Phusion Buffer + $MgCl_2$ (7.5 mM)	6 µl
dNTP mix (10 mM)	0.9 µl	dNTP mix (10 mM)	0.9 µl
Primer F (10 µM)	0.9 µl	Primer F (10 µM)	0.9 µl
Primer R (10 µM)	0.9 µl	Primer R (10 µM)	0.9 µl
DreamTaq DNA Pol. (5U/µl)	0.2 µl	Phusion DNA Pol. (2U/µl)	0.25 µl
DNA template	1 µl	DNA template	1 µl
ddH_2O	23.1 µl	ddH_2O	20 µl
Final volume	30 µl	Final volume	30 µl

The PCR conditions:

Step	Conditions		
	Temperature	**Time**	
Initial denaturation	95°C	3 min	
Denaturation	94°C	30 s	5x
Primer annealing	specific[1]	30 s	
Primer extension	72°C	specific[2]	
Denaturation	**94°C**	**30 s**	30-35x For **Touch-down PCR** the T_a was reduced by 0.4 °C in each cycle
Primer annealing	specific[1]	30 s	
Primer extension	72°C	specific[2]	
Cooling	12°C	∞	

[1] T_m (melting temperature) of primer depends on the primer length and its GC quantity. It usually ranges between 55 – 65 °C. For the first five cycles the T_a was about 2 – 5 °C higher in order to increase primer annealing specificity.

[2] Time of DNA polymerization was set according to the polymerase processivity and the length of amplified fragment. Expected processivity of DreamTaq polymerase is about 1kb for 1 min and processivity of Phusion polymerase is assumed to be about twice as high (www.thermoscientificbio.com).

Some of the constructs (eg. the dRNAs) were cloned (see 4.1.2.1) using the Splicing by Overlap Extension Polymerase Chain Reaction (SOE PCR; Horton, 1995) in combination with Touch-down PCR (Don et al., 1991). During SOE PCR the DNA fragments are linked based on their overlapping ends. Touch-down PCR is a method which helps to avoid amplification of nonspecific sequences. The primer melting point determinates the upper limit of annealing temperature during PCR. Below this point only very specific base pairing between the primer and the template occurs. At lower temperatures the primer binding is even less specific. The annealing temperature is higher in earliest steps of a Touch-down PCR cycle and it progressively decreases for every subsequent set of cycles.

Eight primers (P1 F, P1 R, P2 F, P2 R, P3 F, P3 R, P4 F, P4 R; for sequences see 3.2.4) were designed with overlapping ends complementary to each other for SOE PCR (overlapping depends on the sequence order) and they were used for the first PCR amplification of target sequences. The programme used for primer design was Vector NTI Suite 9.0.0. Some of the primers contained the restriction sites.

3.3.1.3. Horizontal agarose gel electrophoresis

This separation method is used to separate DNA molecules fragments of different length on the basis of their electrophoretic mobility. DNA molecules have polyanion form in neutral or alkaline environment and the number of nucleotides in fragment; therefore the molecule charge increases proportionally. Agarose gel electrophoresis was used in order to separate and visualize PCR products or restriction fragments. It was also used for the excision and isolation of DNA fragments of the desired length from the gel.

Agarose gel of desired concentration (usually 0.8%) was boiled in a microwave and once it was cooled to 55 °C, 1 μl of ethidium bromide (1 mg/ml) was added per 100 ml of melted agarose. After gel solidification the gel was put into a horizontal electrophoresis apparatus Mini-Sub Cell GT and immersed in 1x TAE buffer. Then the molecular marker and samples mixed with a loading buffer were loaded into wells. The applied voltage was 90 V or 100 V for about 35 min. DNA bands were visualized by UV transilluminator and photographed using the documentation system Gel Doc EQ.

The gel plug in front of the migrating fragment was removed and replaced by a low-melting agarose when the fragment was intended to be isolated from the gel and high yields were required. Then electrophoresis was run again in order to allow migration of the fragment into low-melting agar plug.

50x TAE buffer (Tris-acetate-EDTA): 24.2% (w/v) Tris, 10% (v/v), 0.5 M EDTA, 5.7% (v/v) CH_3COOH, pH 8

1% agarose gel: 1% (w/v) agarose diluted in 1x TAE buffer with 1 μl of ethidium bromide (1 mg/ml)

1.5% low-melting agarose gel: 1.5% (w/v) low melting agarose diluted in 1x TAE buffer with 1 μl of ethidium bromide (1 mg/ml)

Loading buffer: 6x DNA Loading Dye (Fermentas, USA)

DNA molecular marker: GeneRuler™ 1 kb DNA Ladder and GeneRuler™ 100 bp DNA Ladder (Fermentas, USA). Both markers were mixed with loading buffer and dissolved in ddH_2O in appropriate ratio.

3.3.1.4. DNA fragment isolation from agarose gel

For DNA isolation from agarose the commercial High Pure PCR Product Purification Kit was used. The principle of this kit is based on the DNA selective binding to special silicate fibers in the presence of chaotropic agents (guanidine thiocyanate). Following DNA elution is performed by a solution with low ionic strength and alkaline pH. The entire protocol was performed according to the kit instructions.

Agarase enzyme digestion of low melting agar was used to avoid DNA loss frequently associated with commercial column based isolation procedures (High Pure PCR Product Purification Kit), especially when working with long DNA fragments (10 kb and above). The excised gel block with sample was thawed at 83 °C for 5 min and then tempered at 42 °C. Then 1 µl of agarase (0.5 U/µl) was added to 100 µl of gel and sample was incubated at 42 °C for 30 min.

The isolated DNA concentration was then measured on NanoDrop 1000 Spectrophotometer.

3.3.1.5. DNA precipitation

When the DNA concentration in a sample was too low, the precipitation and solution in a smaller volume of buffer was made according to the following protocol:

1. Adjust the total sample volume to 200 µl by ddH_2O.
2. Add 20 µl 3M NaOAc (pH 5.2) and 400 µl 95% EtOH.
3. Leave to precipitate in refrigerator overnight or in deep freezer (-80 °C) for at least 30 min.
4. Centrifuge for 15 min at maximum in a table centrifuge (Biofuge Pico, 16060 g).
5. Wash twice with 400 µl 75% EtOH, let stand for 10 min and then again centrifuge for 5 min.
6. Dry the sample at 42 °C in thermo block and dilute in a small volume of ddH_2O or commercial EB buffer (Qiagen, Germany).

3.3.1.6. DNA restriction

The specific restriction endonucleases (RE) were routinely used both for subcloning of recombinant constructs and/or for their verification. RE are derived from bacteria with ability to restrict foreign DNA in specific sequences, called a restriction sites. The reaction

mixture was mixed according to instructions for each RE. See a typical reaction in the following table:

Component	Volume	Conditions
Appropriate NEB buffer 10x	2 µl	37 °C for at least 3 h in the case of classic enzymes
RE 1	2-3 U	
RE 2	2-3 U	
BSA 100x (10 mg / ml)	0.5 µl	
DNA plasmid (about 200 ng / µl)	5 µl	
H_2O	Y µl	
Total volume	20 µl	

[1] RE volume depends on the enzyme concentration (in U/µl). One unit (U) is defined as the amount of enzyme required to digest 1 µg of DNA in 1 hour at 37 °C in a total reaction volume of 50 µl.

After reaction the REs must be deactivated by heating (usually 75 °C, 10 min) or by purification (High Pure PCR Product Purification Kit) depending on the enzymes used.

3.3.1.7. DNA dephosphorylation and ligation

In most cases of subcloning, a combination of two RE was used (where at least one RE generates cohesive ends) which increased the rate of successful cloning of the fragment in the correct orientation and reduced plasmid self-ligation. In cases when the linearized plasmid contained compatible ends, they had to be dephosphorylated after restriction in order to reduce plasmid self-ligation. The dephosphorylation was also frequently used in incompatible ends cloning procedures, where it still improves background arising from inefficient digestion.

The following protocol was used:

1. Restriction reaction (see 3.3.1.6).
2. Dephosphorylation of linearized plasmid:
   Add to deactivated restriction mix 1 µl SAP (1U/µl) and incubate at 37 °C for 15 min (SAP should be fully active in all NEB restriction buffers).
3. REs and SAP deactivation at 75 °C for 20 min.
4. Typical ligation mixture:
   - 1 µl of plasmid[1]/deactivated restriction reaction
   - 1 µl inzert[1]/deactivated restriction reaction

- 1 µl T4 DNA ligase buffer 10x
- 1 µl PEG 4000 (50%, w/v)
- 5 µl dH_2O or increase the total volume to 20 µl
- 1 µl T4 DNA ligase (5 U / µl)

5. Place the microtubes with reaction mix on water bath (room temperature) and leave to ligate in a refrigerator (4 °C) overnight or at least 3 hours.
6. DNA ligase deactivation at 75 °C for 10 min.
7. Transformation of *E. coli* bacterial strain.

[1] Recommended molar ratio is about 1:3 (plasmid: insert).

3.3.1.8. TA cloning

Some DNA polymerases, such as DreamTaq polymerase, have the ability to generate DNA molecules with single base 3´end overhang (mostly adenosine; Clark, 1988). This DNA molecule can be used for ligation of the PCR product into the linearized vectors with one base thymine extension on the 3´end, such as commercial plasmid pTZ57R / T (see Figure 6).

TA cloning was initiated with PCR amplification followed by purification of PCR product by High Pure PCR Product Purification Kit. Then the purified PCR product was ligated into pTZ57R/T plasmid according to the protocol (see 3.3.1.7) followed by transformation of *E. coli* (see 3.3.2.1).

3.3.1.9. In-Fusion cloning

The cloning protocol of the In-Fusion Advantage PCR Cloning Kit was used in case that the cloning via restriction and ligation failed. The principle of the In-Fusion cloning is based on that the sense and antisense primers that are used to amplify the fragment of interest must contain a specific 15 nucleotide sequence which is homologous to the ends of linearized vector. During incubation, the "In-Fusion Enzyme" contains viral recombinase that specifically recognizes and recombines these short homologous stretches of DNA and guarantees a high percentage of correctly cloned molecules. The drawback of the technique is, that the plasmid DNA in the reaction mixture has to be highly concentrated – approximately 200 ng of digested and purified DNA is used per reaction.

For our purposes, primers Inf#1 F and Inf#4 R were designed (see 3.2.4). The entire protocol was performed according to the kit instructions.

3.3.1.10. Sequencing

All cloned PCR fragments as well as all newly constructed infectious clones were verified by sequencing. Most sequencing reactions were performed by GATC Biotech AG, Germany. The obtained chromatograms were processed in the Vector NTI Advance 11 programme (application ContigExpress).

3.3.1.11. RNA isolation from viral particles

RNA was isolated from the plant extract samples where the degradation of RNA unprotected by viral capsid was assumed. The goal was to isolate RNA from viral particles. Modified protocol was applied as described for RNazol RT Kit:

1. DNA/protein precipitation: mix 100 µl plant extract in PBS (see 3.3.5.3), 250 µl cold RNazol RT and 140 µl dH_2O and wait 15 min. Then centrifuge for 15 min at maximum in a table centrifuge (Biofuge Pico, 16060 g).
2. RNA precipitation: mix 200 µl supernatant with 450 µl 75% EtOH, wait 10 min and centrifuge again for 8 min.
3. RNA washes: wash twice the pellet with 200 µl 75% EtOH and centrifuge for 3 min.
4. RNA solubilization: dry the pellet at 37 °C in thermo block and dissolve in 20 µl dH_2O.

The isolated RNA concentration was then measured on NanoDrop 1000 Spectrophotometer.

3.3.1.12. Reverse transcription

Isolated RNA was transcribed to cDNA (complementary DNA) for subsequent sequence analysis by PCR.

Modified protocol was applied as described for M-MLV Reverse Transcriptase:

1. Primer annealing reaction mix:
    - 1 µl TMV-3´NTR R primer (10 µM)
    - 5 µl M-MLV RT 5x Buffer
    - X µl RNA (to achieve 1.5 µg RNA in reaction)
    - Y µl dH_2O (adjust the total volume to 15 µl)

    Incubate samples at 70 °C for 10 min in PCR cycler. Add components as listed in the following step:

2. Reverse transcription:
    - 1 µl dNTP mix (10 mM)
    - 0.5 µl RiboLock RNase Inhibitor (40 U/µl)
    - 1 µl M-MLV RT (200 U/µl)
    - 7.5 µl dH_2O to total volume 25 µl

    Incubate samples at 40 °C for 60 min in PCR cycler. Resulting cDNA can be used as the PCR template.

3.3.2. Bacterial transformation and cultivation

3.3.2.1. *E. coli* transformation and cultivation

Chemical transformation of competent *E. coli* cells was performed according to the below described protocol:

1. Thaw competent cells and inactivate ligation reaction/In-Fusion reaction on ice.
2. Mix 100 µl competent cells with 5 µl ligation reaction/1 µl In-Fusion reaction in microtube and incubate 30 min on ice.
3. Heat shock cells at 42 °C for 45 s in thermo block and replace on ice for 2 min.
4. Add 500 µl LB medium without antibiotic and incubate 30 min at 37 °C in the shaking incubator.
5. Centrifuge the tubes shortly in the table centrifuge, remove most of the supernatant, resuspend cells in about 150 µl LB medium and spread over the plate with LB agar with selection antibiotic.
6. Incubate plates overnight at 37 °C or 36 - 48 hours at 28 °C[1].

[1] The temperature of 28 °C was preferred for infectious full-length constructs, because they exhibit better stability at lower temperatures.

For the purposes of DNA isolation and selection of bacterial clones, the bacteria were incubated in 4 ml LB medium with antibiotic overnight at 37 °C or at 28 °C for 36 – 48 hours in the shaking incubator. Plasmid DNA was purified using QIAprep Spin Miniprep Kit.

LB medium: 1% (w/v) peptone, 0.5% (w/v) yeast extract, 171 mM NaCl

LB agar: 1% (w/v) peptone, 0.5% (w/v) yeast extract, 1.6% (w/v) bacto-agar, 171 mM NaCl

Antibiotics	Final concentration	Selection marker for:
Kanamycin	30 μg/ml	pGR2 and pGR plasmids
Carbenicillin	150 μg/ml	pTZ57R/T, pGEM

Table 1: Antibiotic concentrations used.

3.3.2.2. *A. tumefaciens* transformation and cultivation

A chemical transformation of competent GV3101 *A. tumefaciens* cells was performed according to the following protocol:

1. Thaw competent cells and DNA isolated from bacteria on ice.
2. Mix 100 μl of competent cells with 1 μg of plasmid in microtube.
3. Freeze in liquid nitrogen for about 5 min.
4. Thaw the tubes at 37 °C in thermo block then re-freeze in liquid nitrogen.
5. Once again thaw the tubes at 37 °C in thermo block and then incubate on ice for 5 min.
6. Add 500 μl LB medium without antibiotic and incubate 30 min at 28 °C in the shaking incubator.
7. Centrifuge the tubes shortly in the table centrifuge, remove most of the supernatant, resuspend cells in about 150 μl LB medium and spread over the plate with LB agar with 30 μg/ml kanamycin.
8. Incubate plates 36 - 48 hours at 28°C.

Grown colonies can be inoculated into 4 ml liquid LB medium with 30 μg/ml kanamycin. After 36 – 48 hours of growing at 28 °C in the shaking incubator, the cells can be used for plant agroinfiltration (see 3.3.4.1).

For long-term storage of the verified clones, the glycerol stocks were made according to the following protocol:

1. Take 500 μl of liquid culture growing at an exponential phase and centrifuge for 1 min at maximum in a table centrifuge. Remove the medium and resuspend cells in 500 μl fresh LB medium with antibiotic.
2. Add 500 μl of 50% glycerol, mix gently and freeze in liquid nitrogen.
3. Store in a deep freezer at -78 °C.

3.3.3. Plant cultivation

Plants have grown in autoclaved soil mixed with 1/10 of silica sand under a controlled light cycle of 14 hours of light and 10 hours of dark at the constant temperature of 22 °C in an air-conditioned growth room. After the infection was conducted, the plants were moved to the controlled conditions of 23 °C with light cycle 14 hours of light (programme 4) and 10 hours of dark in SANYO growth incubators. Some of the infected plants selected for particle-assembly under higher temperature experiment were planted in SANYO growth incubator under the same light conditions but with the temperature of 33 °C.

3.3.4. Plant inoculation

3.3.4.1. Agroinfiltration

Agrobacterium tumefaciens is a gram-negative bacterium naturally infecting dicotyledonous plants. An infection with *Agrobacterium* leads to a tumour formation caused the bacterial DNA (transfer DNA, T-DNA) integration into the plant genome. T-DNA contains genes for plant growth factors and enzymes providing a source of carbon and nitrogen for bacterium. T-DNA is contained within the Ti-plasmid (Tumour-inducing plasmid), situated between so-called “right border” (RB) and “left border” (LB) sequences and its size ranges between 10 - 30 kbp. Bacterial chromosomal genes and Ti-plasmid virulence genes are important for the T-DNA transfer (Tzfira & Citovsky, 2008).

The plants were inoculated according to the following protocol:

1. Centrifuge the tubes with a grown *Agrobacterium* culture for 10 min at 3500 g (Multifuge 3S-R, 6445 rotor).
2. Replace medium with fresh LB induction medium (LB + 30 μM kanamycin + 100 μM acetosyringone) and incubate the tubes at 28 °C in a shaking incubator for at least 3 hours.
3. Centrifuge the tubes again as above, replace the medium and resuspend the cells in the infiltration medium.
4. Dilute to the absorption about $A_{600} = 0.7$.
5. Inoculate the solution into the abaxial side of completely developed *N. bentamiana* leaves by gentle injection with a sterile syringe without a needle.
6. Place plants under controlled conditions in SANYO growth incubator[2].

During the coinoculations we have used 1:1 ratio of helper and dRNA construct cultures. Plants were harvested usually 7 – 10 days *post* infection (dpi).

[2] In case of the particle-assembly under higher **temperature experiment**, the plants were moved from 23 °C to 33°C two days after the infiltration.

Infiltration medium: 10 mM MES, 10 mM $MgCl_2$, 100 μM acetosyringone (100 mM stock solution in DMSO) in dH_2O.

3.3.4.2. Mechanical plant inoculation with virions

This inoculation method was used to confirm the presence of infective particles in the plant extract from agroinfiltrated plants. The infected *Nicotiana bentamiana* plants exhibited various symptoms depending on the infective particles presence in the extract. Infected *Nicotiana tabacum*, cv. Samsun NN showed local necrotic lesions of typical hypersensitive response upon challenge with infectious particles.

The inoculation procedure was very simple: the adaxial side of completely developed leaves was lightly dusted with carborundum powder and about 10 μl of plant extract (see 3.3.5.2) was applied per each leaf. Subsequently, the extract with carborundum was rubbed on leaf area by a gloved finger. The plants were then moved under the controlled conditions in SANYO growth incubator. The plants were harvested usually 7 – 10 days *post* infection (dpi).

3.3.5. Protein methods

3.3.5.1. TMV isolation and purification

The initial TMV-U1 strain purificate was obtained from Mgr. Tomáš Moravec, Ph.D. This purificate was inoculated to *Nicotiana tabacum* plants and leaves were harvested and processed at 7 dpi. Resulting purified virus preparation was used as a positive control in the following protein methods (SDS-PAGE, WB), and its dilution aliquots were used as a viral protein quantity indicator in the plant extracts.

TMV purification protocol:

1. Add one volume of infected leaves to three volumes of extraction buffer and put it into a blender for about 3 min.
2. Filter through silk and centrifuge for 10 min at 9500 g (Sigma 3K30, rotor 12150-H) at 5 °C in 50 ml falcon tubes.

3. Decant the supernatant with care through silk and add NaCl to the 3% and PEG 6000 to the 5% final concentration. Leave it to dissolve on a magnetic mixer and then place to a refrigerator overnight in order to precipitate most of the TMV particles.
4. Centrifuge again for 15 min at 9500 g in 50 ml falcon tubes.
5. Remove supernatant and crystallized material from the pellet and properly resuspend the pellet in about ¼ of original volume of 50 times diluted extraction buffer.
6. Centrifuge for 15 min at 9500 g in 50 ml falcon tubes.
7. Load the supernatant on the 20% sucrose cushion (in the same 50x extraction buffer) in centrifugation cuvettes and centrifuge for 3 hours at 88000 g (Ultracentrifuge Beckman L7-55, rotor Ti50.2).
8. Remove the supernatant and gently wash the pellet from chlorophyll. Then resuspend the pellet in a PBS buffer (see 3.3.5.3)

The absorbance spectrum between 220 – 300 nm was then measured on HEλIOS γ spectrophotometer. The concentration of the purified virus was calculated using the formula: c [mg/ml] = (A_{260} . dilution) / ${}_{E}K_{(TMV)}$. The TMV extinction coefficient (${}_{E}K_{(TMV)}$) is 3.

Extraction buffer: 2.46 g NaH_2PO_4 . 2 H_2O + 12.24 g Na_2HPO_4 . 12 H_2O + 0.5 g ascorbic acid in 100 ml dH_2O, pH 7.2

3.3.5.2. Protein separation by SDS-PAGE

SDS-PAGE (SDS-Polyacrylamide Gel Electrophoresis) is used for the separation of proteins according to their apparent molecular weight. Negatively charged sodium dodecyl sulphate (SDS) detergent binds to proteins at a constant rate (approximately 1.4 g SDS per 1 g of protein). Since the electric charge is mostly conferred by SDS ions and is thus independent of the protein sequence, the apparent electrophoretic mobility is only dependent on protein size.

SDS-PAGE was used to detect and compare the levels of accumulated TMV CP in the plant extracts. The same plant extract in phosphate buffer was generally used for SDS-PAGE, Western blotting, RNA isolation and electron microscopy.

The plant extract preparation was performed as below:

1. 24 – 26 mg of plant biomass from inoculated leaves or from non-inoculated young upper leaves were collected into a tube with ceramic grinding beads, and 400 µl of PBS was added to each tube.

2. Samples were homogenized in FastPrep-24 homogenizer for 40 s.
3. Plant debris was removed by centrifugation for 1 min at maximum speed in a table centrifuge (Biofuge Pico, 16060 g).
4. About 250 µl of supernatant was recovered and stored at -20 °C for further analysis.

Electrophoresis was performed in a Mini Wide Vertical Gel Electrophoresis Apparatus according to (Laemmli & others, 1970). During the migration in stacking gel 120 V was applied while the voltage was increased to 150 V in resolving gel. Since the TMV CP is a relatively small protein of 17.5 kDa, 15% resolving gel was used thorough the whole work. Polyacrylamide gels were then stained by SimplyBlue SafeStain (Coomasie G-250) according to the commercial staining protocol.

The composition of the gels:

Component	**15% Resolving gel**	**5% Stacking gel**
Redistilled H_2O	5 ml	6.3 ml
Buffer 1	3.5 ml	-
Buffer 2	-	2.5 ml
40 % Acrylamid/Bis	5.3 ml	1 ml
10% SDS	140 µl	100 µl
10% APS	105 µl	94 µl
TEMED	14 µl	20 µl
One gel total volume	14.06 ml	10.01 ml

The SDS-PAGE sample preparation:

1. Mix plant extract sample with sample buffer in 1:1 ratio.
2. Protein denaturation at 65 °C for 10 min.
3. Centrifuge for 1 min at maximum in a table centrifuge (Biofuge Pico, 16060 g), and load samples on the gel.

Phosphate buffer (PBS, Phosphate Buffered Saline): 137 mM NaCl, 7.8 mM Na_2HPO_4 . 12 H_2O, 1.5 mM KH_2PO_4, 2.7 mM KCl, 3.1 mM NaN_3, pH 7.4

Buffer 1: 1.5 M Tris-HCl, pH 8.8

Buffer 2: 0.5 M Tris-HCl, pH 6.8

Sample buffer (Laemmli buffer): 62.7 mM Tris-HCl, 69.3 mM SDS, 0.64 M mercaptoethanol, 0.3 M sucrose, 0.03 M bromphenol blue

Electrode buffer: 25 mM Tris, 188 mM glycin, 3.5 mM SDS

Marker Spectra Multicolor Broad Range Protein Ladder (Thermo Scientific, USA)

3.3.5.3. TMV coat protein immunodetection

This method is based on the transfer of proteins from polyacrylamide gel onto a nitrocellulose membrane and a subsequent detection of the protein of interest by specific antibodies. A protein transfer from polyacrylamide gel onto a nitrocellulose membrane (**Western blot, WB**) was performed according to the following protocol:

1. SDS-PAGE (see 3.3.5.2).
2. Prepare 6 filter papers (Munktell, Bio-Sciences AB, Sweden) and nitrocellulose transfer membrane (Whatman, Protran, Germany) cut in the dimensions of the polyacrylamide gel and moistened in the transfer buffer, as well as the Western blot apparatus electrodes.
3. Put layers in the following order on the WB apparatus cathode: three filter papers, polyacrylamide gel (washed in dH_2O), nitrocellulose membrane, three filter papers, and enclose by WB apparatus anode.
4. Electroblotting transfer at 0.8 mA/cm^2 for 1.5 hour.

Protein immunodetection on nitrocellulose membrane:

1. Wash the nitrocellulose membrane in dH_2O and then non-specifically dye proteins with Ponceau S solution. Wash again and take a photo of the membrane.
2. Membrane blocking: immerse the membrane into 5% non-fat milk solution in PBS for 1 hour in order to prevent the interactions between the membrane and the antibody used for detection of the target protein.
3. Incubate the membrane with anti-TMV primary polyclonal rabbit antibody overnight (antibody diluted in a washing buffer in a ratio of 1:1 500) in Hybridiser HB-1D Incubator at 27 °C.
4. Wash the membrane three times in the washing buffer for 5 min.
5. Incubate the membrane with anti-rabbit secondary goat antibody labelled by alkaline phosphatase for 2.5 hours (antibody was diluted in the washing buffer in a ratio of 1:30 000) in Hybridiser HB-1D Incubator at 27 °C.
6. Wash the membrane three times in the washing buffer for 5 min.

7. Incubate the membrane in the substrate BCIP/NBT solution. When the sufficient signal is achieved, dry the membrane and take a photo.

Transfer buffer: 25 mM Tris, 188 mM glycin, 20% (v/v) methanol

Ponceau S solution: 30% (w/w) trichloracetic acid, 30% (w/w) sulfosalicylic acid, 2% (w/v) Ponceau S

Washing buffer: 137 mM NaCl, 7.8 mM $Na_2HPO_4.12\ H_2O$, 1.5 mM KH_2PO_4, 2.7 mM KCl, 3.1 mM NaN_3, 0.05% (v/v) Tween 20, pH 7.4

Phosphate buffer (PBS): 137 mM NaCl, 7.8 mM $Na_2HPO_4.12\ H_2O$, 1.5 mM KH_2PO_4, 2.7 mM KCl, 3.1 mM NaN_3, pH 7.4

3.3.6. Fluorescence microscopy and observation

The LED diodes with emission maximum of 390 – 405 nm with green or yellow filters were used in order to detect GFP expression in inoculated plants. The images of whole plants were recorded using Olympus E-510 digital camera and Zeiss 35/2.4 lens. Microscopic photos of inoculated leaves were taken using Leica DM 5000B fluorescence microscope with GFP specific filter cube and Leica DFC490 color digital camera. The GFP emission maximum is around 510 nm.

3.3.7. Transmission electron microscopy (TEM)

Direct proof of the presence of viral particles in plant extract is their visualization using transmission electron microscope. The FEI Morgagni 268D Transmission Electron Microscope was used. All particles were photographed at a magnification of 56 000 and subsequently measured and processed in iTEM analysis software (Olympus Soft Imaging Solutions, Germany). Individual measured data sets were inserted into a graph represented distribution of particles in 10 nm intervals. Several data sets measured from one sample were processed in order to verify the robustness of the method.

3.3.7.1. Negative staining of viral particles

Appropriate TEM grids were coated with formvar film prior to the staining procedure.

Grid coating with formvar film was done as follows:

1. Put few drops of diluted detergent on the microscopic glass slide and polish with lint-free paper napkin.
2. Immerse the slide into 2% formvar solution (in chloroform). The thickness of film depends on the rate of slide removal from the formvar solution.
3. Dry the slide and trim the edges by scalpel.
4. Slowly immerse slide into water bath in order to release the film from the glass and let it float on the water surface. The thickness can be estimated from the colour of the film, best are grey-silver films.
5. Lay the grids (nickel grids, mesh size 300, SPI Supplies, USA) carefully on the film and remove the film with grids from the water surface using a sheet of parafilm (Bemis, USA).
6. Store the formvar coated membranes in Petri dish.

Negative staining protocol used:

In each step the grid was incubated on 15 µl drops of particular solution. Before proceeding to the next step, the grid was carefully taken with antimagnetic forceps and excess liquid was wicked off with a clean filter paper. Thorough the procedure attention was taken to expose the same grid surface to all reagents.

1. Antibody binding: anti-TMV primary polyclonal rabbit antibody (diluted in PBS, 1:30) for 30 min.
2. Washing: PBS for three min, three times.
3. Particle binding: plant extract (see 3.3.5.2) for 30 min.
4. Washing: dH_2O for three min, two times.
5. Staining: 4% ammonium molybdate with 1% trehalose for five min.

4. RESULTS

4.1. Cloning

The proposed system for the production of specific-length particles in plants is based on simultaneous replications of two vectors in a plant cell. The first vector carries a TMV virus modified in such a way that its RNA does not contain encapsidation signal also known as an origin of assembly (OAS). As the OAS is located in the MP gene, this gene has been removed as well, however, all the other viral components required for the replication of viral RNA and production of CP have been maintained. This vector serves as a helper virus. The second vector carries a defective RNA (dRNA) which is dependent on the replication of the helper virus. This construct contains only 5'NTR and 3'NTR terminal viral sequences required for recognition by viral replicase and the RNA replication; the viral OAS necessary for specific recognition of RNA by a viral coat protein and thus for the particle assembly and a reporter sequence (GFP) for easy detection. The length of dRNA determines the length of the resulting particles.

Both construct types were cloned into the T-DNA region of a binary vector pGR2. After T-DNA insertion into a plant genome by *Agrobacterium*, the construct transcription initiation and termination should be guaranteed by regulation elements CaMV 35S promoter and Nos terminator. The **CaMV 35S promoter** from cauliflower mosaic virus is a very strong constitutive promoter, causing high levels of gene expression in dicotyledonous plants (Fang et al., 1989). The **Nos terminator** from the nopaline synthase gene of *Agrobacterium tumefaciens* (Meric et al., 2004) was chosen as an appropriate transcription terminator. The **hammerhead ribozyme** sequence from satellite tobacco ringspot virus (Khvorova et al., 2003) was added downstream the KpnI restriction site and is designed to ensure the formation of natural 3'end of dRNA, reassembling exactly the 3′end of wild-type TMV (Moravec, unpublished). The ribozyme has the ability to cleave itself autocatalytically thus ensuring the shortening of RNA. These sequences are not present in the expressed and processed RNA sequence (see Figure 13, A).

4.1.1. Helper constructs

The pGR2i plasmids were used for helper constructs cloning due to high instability of TMV full-length cDNA clones in pGR plasmids. pGR2i plasmids contain intron ("i" means intron) from *N. tabacum* anionic peroxidase gene (Diaz-De-Leon et al., 1993) in the RdRp ORF.

The main reason for the intron sequence addition was the improved plasmid stability in *E. coli*. It had been described previously, that background expression of replicase protein might be toxic for bacteria (Marillonnet et al., 2005; López-Moya & García, 2000). As an additional advantage, the intron sequence induces RNA processing in nucleoplasma and thus increases the helper-virus RNA stability and transport from the nucleus, improving the efficiency of infection cycle initiation. It is important to note, that natural TMV RNA would never get into the plant nucleus during its infectious cycle.

Helper construct	Lengths of genomic and subgenomic RNAs	Calculated particles length	Particles
TMV-U1	full 6395 nts sgMP 1558 nts sgCP 693 nts	300 nm* 73 nm* 33 nm	TMV-U1
pGR2i-NAGD/CASP	full 6408 nts sgMP 1570 nts sgCP 705 nts	301 nm* 74 nm* 33 nm	TMV-NAGD/CASP
pGR2i-dOAS	full 5841 nts sgMP 1004 nts sgCP 693 nts	274 nm 47 nm 33 nm	TMV-dOAS
pGR2i-dOAS2	full 5780 nts sgMP 943 nts sgCP 693 nts	271 nm 44 nm 33 nm	TMV-dOAS2
pGR2i-dOAS-NAGD/CASP	full 5854 nts sgMP 1017 nts sgCP 706 nts	275 nm 48 nm 33 nm	TMV-dOAS-NAGD/CASP
pGR2i-dOAS2-NAGD/CASP	full 5793 nts sgMP 956 nts sgCP 706 nts	272 nm 45 nm 33 nm	TMV-dOAS2-NAGD/CASP

Table 2: Characteristics of helper constructs RNAs and putative particle size. The known TMV-U1 genome sequence and length (6395 nts; NCBI accession number: NC_001367.1) and the generally reported particle length of 300 nm were used for the particle lengths calculation based on the constructs RNA length. sgCP RNA transcription start (at the 5703 position in TMV-U1 genome) and sgMP RNA transcription start (at the 4838 position, Grdzelishvili et al., 2000) were measured as the first nucleotide of the sgRNAs lengths, the last nucleotide corresponds to the natural TMV-U1 end. The full RNA length was measured from 5´NTR first nucleotide to the natural TMV-U1 end. It is important to note, that (sg)RNAs marked by "*" should be packaged to the particles due to presence of the OAS sequence. To obtain a complete data set, all potential sgRNAs and resulting particle lengths were added as well. However, the sgCP RNA particle assembly was not observed.

The construct **pGR2i-NAGD/CASP** corresponds to the TMV-U1 genome with replicase proteins, a coat protein and also a movement protein, but there is a modification in the CP protein. This modification is situated in the protein inner channel region (amino acids 94 - 106; see Figure 10) and encodes Co and Pt metal binding peptide NAGDHAN (Mao et al., 2004).

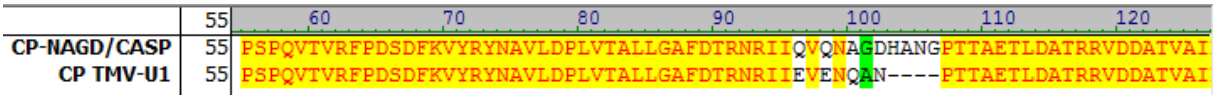

Figure 10: Amino acid sequence alignment of TMV-U1 coat protein and modified coat protein (CP-NAGD/CASP). The full length of the original TMV coat protein is 159 amino acids. Figure was created in Vector NTI Advance 11 programme (AlignX).

The helper construct **pGR2i-dOAS** provides all functions necessary for viral infection cycle except the MP protein. The sequence of this construct corresponds to the TMV-U1 genome but most of the MP ORF was deleted in order to remove encapsidation signal OAS. Only a short central part (with 23 bases from OAS_{75}) and last the 161 bases of MP ORF were preserved in pGR2i-dOAS (see Figure 11). The helper construct **pGR2i-dOAS2** was derived from the pGR2i-dOAS construct. Additional 61 bases from the MP ORF upstream of the NcoI restriction site were removed in the pGR2i-dOAS2. Thus only the NcoI restriction site from OAS_{75} was preserved in this construct (see Figure 11). The RNA produced from the pGR2i-dOAS or pGR2i-dOAS2 constructs does not contain the crucial OAS_{75} sequence AAGAAGUCG which is in context of the RNA secondary structure exposed as a single strand at the apex of loop 1. I have also prepared both variants of "dOAS-constructs" with modified CP-NAGD/CASP (constructs **pGR2i-dOAS-NAGD/CASP** and **pGR2i-dOAS2-NAGD/CASP**).

In order to verify the helper constructs sequence correctness, all constructs were sequenced between BamHI restriction site (in RdRp ORF) and 3´NTR region. A few point mutations in RdRp and CP-NAGD/CASP ORFs were found without effect on amino acid sequences.

```
                                                5562
                                                 ↓
MP-U1           tcggtgtgtattgtttatagaaataatataaaattaggtttgagagagaagattacaaac
OAS             ------------------------------------------------------------
pGR2i-dOAS      ----------aggatatctgaaataatataaaattaggtttgagagagaagattacaaac
pGR2i-dOAS2     ------------------------------------------------------------

                                      NcoI
MP-U1           gtgagagacggagggcccatggaacttacagaagaagtcgttgatgagttcatggaagat
OAS             -tgagagacggagggccatggaacttacagaagaagtcgttgatgagttcatggaagat
pGR2i-dOAS      gtgagagacggagggcccatggaa-----------------------------------
pGR2i-dOAS2     ----------tgtcgaccatggaa-----------------------------------
                          * ********
                                                                      5989
                                                                       ↓
MP-U1           gtccctatgtcgatcaggcttgcaaagtttcgatctcgaaccggaaaaaagagtgatgtc
OAS             gtccctatgtcgatca-------------------------------------------
pGR2i-dOAS      ------------------------------------------------aaaagagtgatgtc
pGR2i-dOAS2     ------------------------------------------------aaaagagtgatgtc
```

Figure 11: Sequential alignment of selected part of MP TMV-U1 with the corresponding parts of the pGR2i-dOAS and pGR2i-dOAS2 constructs. A sequence OAS_{75} has been included in the alignment. The NcoI restriction site is highlighted in green. The crucial OAS_{75} sequence AAGAAGUCG is within the red frame. Sequence numbering ("5562" and "5959") is related to the wt TMV-U1 genome. The position of the MP ORF region corresponds to 4093 – 5709 in the TMV-U1 genome. "*" denotes identical nucleotides in all aligned sequences. The multiple sequence alignment was performed by Clustal Omega 1.2.0. (Sievers et al., 2011) and subsequently adapted.

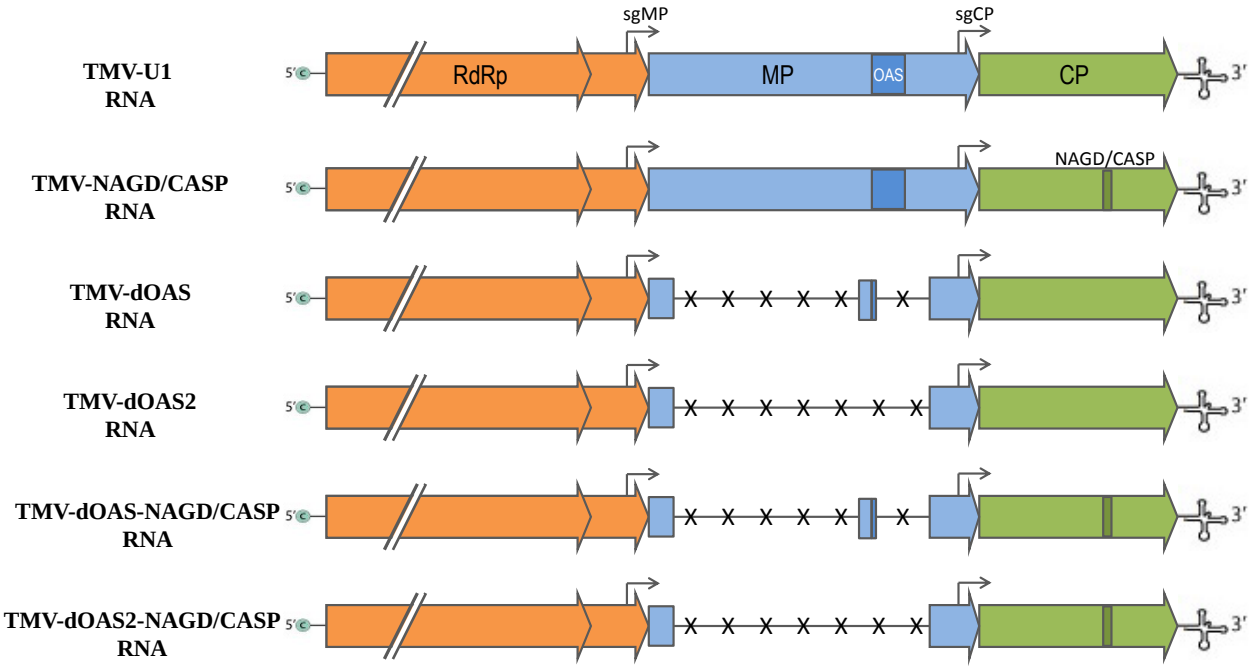

Figure 12: Scheme of RNA sequences of helper viruses. (RdRp; in orange) RNA-dependent RNA polymerase/Replicases, strikethrough indicates shortening of sequences for the image purposes; (MP; in blue) movement protein; (OAS; in dark blue) origin of assembly; (CP; in green) coat protein; (NAGD/CASP) NAGD/CASP epitope; (sgCP and sgMP) subgenomic promoters, note that the sgMP promoter is partly localized in RdRp ORF and sgCP promoter in MP ORF; (X) removed sequences; 5´NTR and 3´NTR are shown at the ends of RNAs.

4.1.1.1. Cloning of helper constructs

The plasmid **pGR2i-dOAS** was assembled by subcloning of NcoI and KpnI digested PCR fragment created using amplification of CP and 3´NTR regions with dOAS F and 4# R primers (see 3.3.1.2). dOAS F primer was designed to eliminate the main part of OAS sequence from the TMV-U1 genome; primer contained NcoI restriction site. Vector pGR-NK2 was used as the template. The resulting fragment was subcloned into the pTZ57R/T plasmid (see 3.3.1.8) and transformed to TOP10 cells (see 3.3.2.1). The selected correct clone and pGR-dMP-IRES plasmid (see Figure 8) were subsequently digested by NcoI and Acc651 REs, and purified fragments were ligated together (see 3.3.1.6 and 3.3.1.7). In order to obtain construct in pGR2 vector, the subcloning to pGR2i-dCP-GFP via BamHI and PstI restriction sites followed.

To remove the remainder of the OAS region, the construct **pGR2i-dOAS2** was constructed using newly designed primer dOAS2 R. This primer contains NcoI and SalI restriction sites at the 5´-end. The fragment from the pGR2i-dOAS template was then amplified by TMV -Rep3148 F and dOAS2 R primers (see 3.3.1.2). The resulting fragment was subcloned into the pTZ57R/T plasmid (see 3.3.1.8) and transformed to TOP10 cells (see 3.3.2.1). The selected correct clone and pGR2i-dOAS plasmid were subsequently digested by BamHI and NcoI REs. Purified fragments were then ligated together (see 3.3.1.7).

The construction of a **pGR2i-NAGD/CASP** vector was performed by In-Fusion cloning (see 3.3.1.9). Available primers, Inf#1 F and Inf#4 R, were used in the PCR reaction with a pGEM-NAGD/CASP vector as the template. This vector contains sequence of modified TMV CP and adjacent viral sequences. Vector pGR2i-dCP-GFP linearized by NcoI and KpnI restriction and subsequently purified served as the target cloning vector.

The “dOAS” versions with modified CP-NAGD/CASP, pGR2i-dOAS-NAGD/CASP and pGR2i-dOAS2-NAGD/CASP, were created by subcloning of a NcoI - KpnI fragment from pGEM-dOAS-NAGD/CASP into corresponding linearized full-length vectors (see 3.3.1.6 and 3.3.1.7).

4.1.2. dRNA constructs

In order to find out the optimal dRNA construct with high RNA production and the ability to be packaged by CP, we designed five constructs of different lengths and cloned them to pGR2 plasmid. All five constructs contained regulation elements CaMV 35S promoter, Nos terminator and Hammerhead Ribozyme similarly to the helper constructs. The only retained viral sequences in expressed dRNA are **5´NTR**, **3´NTR** and **OAS**. Then the **Green fluorescence protein (GFP)** sequence was added as a reporter gene to indicate a successful transformation of the cells and high levels of dRNA in the cytoplasm. Also, since the GFP is not normally present in the TMV genome, it can be used for RT-PCR quantification in a mixture containing both the TMV-helper particles and encapsidated dRNA particles. The GFP region was flanked with SphI and XhoI restriction sites in all constructs to simplify the exchange of GFP with another sequence of interest. The **origin of assembly (OAS)** is known to be a sufficient condition for particle assembly. The main 75 nucleotides sequence of OAS (OAS_{75}), determined by Turner et al. (1988) was used.

While all dRNA constructs contain all above mentioned sequences, they differ mainly in the presence and length of the replicase fragment left between TMV 5´NTR region and GFP coding sequence. Vector **pGR2-GFP (dRNA 1)** is the simplest variant of dRNA-constructs (see Figure 13), where the GFP region follows the 5´NTR region immediately. Contrary to some of the other constructs (pGR2-Rep_{378}-sgCP-GFP/dRNA3 and pGR2-Rep_{778} sgCP-GFP/dRNA5), pGR2-GFP does not contain the minimal subgenomic CP (sgCP) promoter upstream of the GFP sequence, so it is expected to produce lower levels of GFP. The advantage of this approach is that it produces dRNA of one single length, while the constructs that include sgCP do produce and package RNA of two different lengths.

The remaining constructs vary in the length of viral replicase fragment between 5´NTR and GFP. The construct **pGR2-Rep_{378}-GFP (dRNA 2)** contains the first 378 nucleotides of TMV RdRp (this corresponds to a naturally occurring SphI restriction site). The **pGR2-Rep_{778}-GFP (dRNA 4)** construct contains a longer RdRp fragment of 778 nucleotides. The constructs **pGR2-Rep_{378}-sgCP-GFP (dRNA 3)** and **pGR2-Rep_{778}-sgCP-GFP (dRNA 5)** contain an additional sgCP promoter (see Figure 13) driving the transcription of the GFP coding sequence, as mentioned previously.

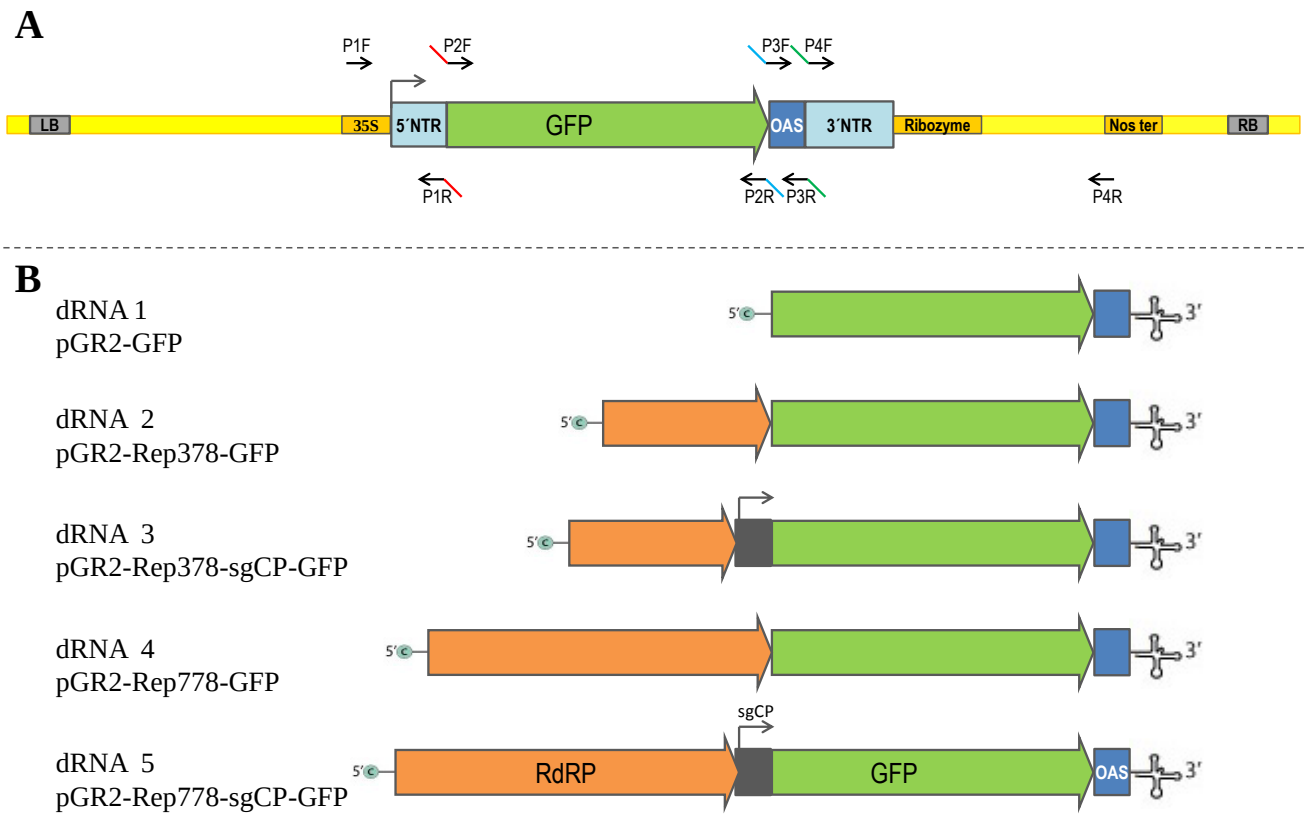

Figure 13: Schematic diagram of dRNA sequences. (A) T-DNA region of the pGR2-GFP construct. Regulation elements 35S promoter, hammerhead ribozyme and Nos terminator shown within the orange frame. Right border (RB) and left border (LB) sequences shown within the grey frame. Primers used for dRNA 1 constructions shown as arrow. **(B)** Scheme of the dRNA sequences: (GFP; in green) green fluorescence protein; (RdRp; in orange) first 378 or 778 nucleotides of RNA-dependent RNA polymerase/Replicases sequence; (OAS; in dark blue) origin of assembly; (sgCP; in grey) subgenomic CP promoter; 5´NTR and 3´NTR are shown at the ends of RNAs or within the light blue frame in the picture 13 A.

dRNA construct	dRNA length	Calculated particle lengths
dRNA 1	1078 nts	51 nm
dRNA 2	1454 nts	68 nm
dRNA 3	1562 nts 1047 nts*	73 nm 49 nm
dRNA 4	1901 nts	89 nm
dRNA 5	2021 nts 1047 nts*	95 nm 49 nm

Table 3: Lengths of produced dRNAs and calculated lengths of putatitive particles. The known TMV-U1 genome length (6395 nts) and the reported particle length of 300 nm were used for particle length calculations based on the dRNA length. dRNA starts at the 35S transcription start (which corresponds to the start of the 5´NTR in dRNA constructs, (Fang et al., 1989) and terminates at the end of the 3´NTR region. dRNA 3 and dRNA 5 produce shorter sgRNA, labelled "*", resulting from the transcription from the sgCP promoter by viral replicases. It is expected, that these sgRNAs accumulate to much higher levels than their corresponding full dRNA.

4.1.2.1. Cloning of dRNA constructs

The basic proposed dRNA construct comprises 4 independent segments of DNA (5´NTR, GFP, OAS_{75} and 3´NTR) and regulation elements (35S promoter, Nos terminator and Ribozyme). In order to assemble these sequences (see 4.1), the following procedures were carried out:

The target sequences amplification was performed in four PCR reactions (see 3.3.1.2) using DreamTaq polymerase. The PCR conditions were following: primer annealing temperature - 52 °C; 57 °C for the first 5 cycles; primer extension time – 45 s for fragments 1 and 2; 22 s for fragments 3 and 4. Four PCR reactions were performed according to the table below:

Fragment	Template	Primers	Restriction site	Sequences present in PCR product	Length
1	pGR-dCP-GFP	P1 F P1 R	- SphI	35S promoter TMV 5´NTR	505 bp
2	pGR-dCP-GFP	P2 F P2 R	SphI XhoI	GFP	772 bp
3	pGR-dCP-GFP	P3 F P3 R	XhoI -	TMV OAS	112 bp
4	pGR-dMP-IRES	P4 F P4 R	- -	TMV 3´NTR Ribozyme	279 bp

The length of the PCR products was checked by horizontal agarose gel electrophoresis (see 3.3.1.3) and DNA fragments of the correct length were isolated from the gel (see 3.3.1.4). Subsequently one more reaction of SOE PCR in a combination with Touch-down PCR was performed. The four isolated fragments from the previous PCR were used as templates in this reaction and PCR conditions were following: primer annealing temperature - in the range of 65 – 55 °C, the temperature decrease of 0.4°C in each cycle; primer extension time – 1 min 35 s. The PCR product of 1557 bp was purified from the gel, then subcloned to the pTZ57R/T by TA cloning (see 3.3.1.8), transformed into DH5α cells (see 3.3.2.1) and verified by sequencing.

The target fragment from pTZ57R/T was subcloned into a pGR2i-dCP-GFP plasmid (see Figure 9) by restriction, fragment isolation from low melting agarose (see 3.3.1.4) and subsequent ligation (see 3.3.1.7). The subcloning via EcoRV and Acc65I restriction has

created the **pGR2-GFP** plasmid and the **pGR2-Rep$_{378}$-GFP** plasmid was obtained by subcloning *via* SphI and Acc65I restriction.

In order to prepare the third plasmid **pGR2-Rep$_{378}$-sgCP-GFP**, the fragment amplified by TMV-sgCP F and P2 R primers from pGR-dCP-GFP template was cloned to the pTZ57R/T plasmid by TA cloning (see 3.3.1.8). A fragment from the selected correct clone was subcloned into pGR2-Rep$_{378}$-GFP plasmid by restriction via SphI and XhoI restriction sites and ligation (see 3.3.1.6 and 3.3.1.7).

Moreover, two plasmids with extended replicase sequence were prepared. Replicase fragment was amplified using primers TMV-sgCP F and P2 R from the plasmid pGR2i-dCP-GFP and subcloned to the to the pTZ57R/T plasmid by TA cloning (see 3.3.1.8). Fragment from selected sequenced correct clone was digested by SphI restriction and subcloned to the SphI linearized plasmids pGR2-Rep$_{378}$-GFP and pGR2-Rep$_{378}$-sgCP-GFP. Resulting plasmids were named **pGR2-Rep$_{778}$-GFP** and **pGR2-Rep$_{778}$-sgCP-GFP** respectively.

The selection of the correct clones was performed by a restriction analysis and sequencing of regions between the 5´NTR and 3´NTR.

4.2. Plant inoculations, symptoms and infectivity of constructs

A. tumefaciens infiltration was used to introduce all dRNA- and helper constructs into plant cells. The ability to cause symptoms or to express GFP reporter protein in host plants was investigated first in order to verify infectivity of constructs. The plants were then coinoculated with selected combinations of the helper and dRNA constructs. The symptoms and a GFP production were observed as well.

The viability of **dRNA constructs** was confirmed by the GFP production in host cells (see Figure 14). It was investigated using 3H or K7 plants (see 3.2.8) coinoculated with the pGR2i-TMV-dCP construct (in a ratio 4:1.5) due to dRNA constructs self-replication deficiency. The pGR2i-TMV-dCP construct contains a TMV genome sequence with a CP ORF deletion so the replication ability is maintained, but there is no CP production and thus no particle packaging. The visual presence of GFP was demonstrated by dRNA 3 and dRNA5 constructs. The GFP production in infected leaves was so high that it was visible even by naked eye after UV illumination. There was no or too low positive signal for the other constructs. Construct pGR2i-dCP causes symptoms in plants itself, so all coinoculated plants showed signs of chlorosis, wilting and mosaic symptoms at agroinfiltrated leaves.

The viability of the **helper constructs** was initially investigated by visual observation of symptoms (see Figure 15). All helper constructs are replication-independent in plant hosts providing MP protein (3H and K7 plants) except pGR2i-NAGD/CASP construct which produces MP itself and thus is infectious even for wt plants. Young plants agroinfiltrated with pGR2i-dOAS and pGR2i-dOAS2 began to wilt. Symptoms as chlorosis and deformed young upper non-inoculated leaves were manifested as well. If the temperature after agroinfiltration was increased to 33 °C, the symptoms were similar with faster progression. Plants agroinfiltrated with pGR2i-NAGD/CASP had similar symptoms accompanied by necrosis on infected leaves. The infection was lethal for the plants exposed to 33 °C temperature – the plants withered due to vascular damage. No visible symptoms were observed on the MP transgenic plants agroinfiltrated with the pGR2i-dOAS-NAGD/CASP or pGR2i-dOAS2-NAGD/CASP constructs even at the temperature of 33 °C. However, infected plants were older, so the symptoms could be mild and masked by plant senescence.

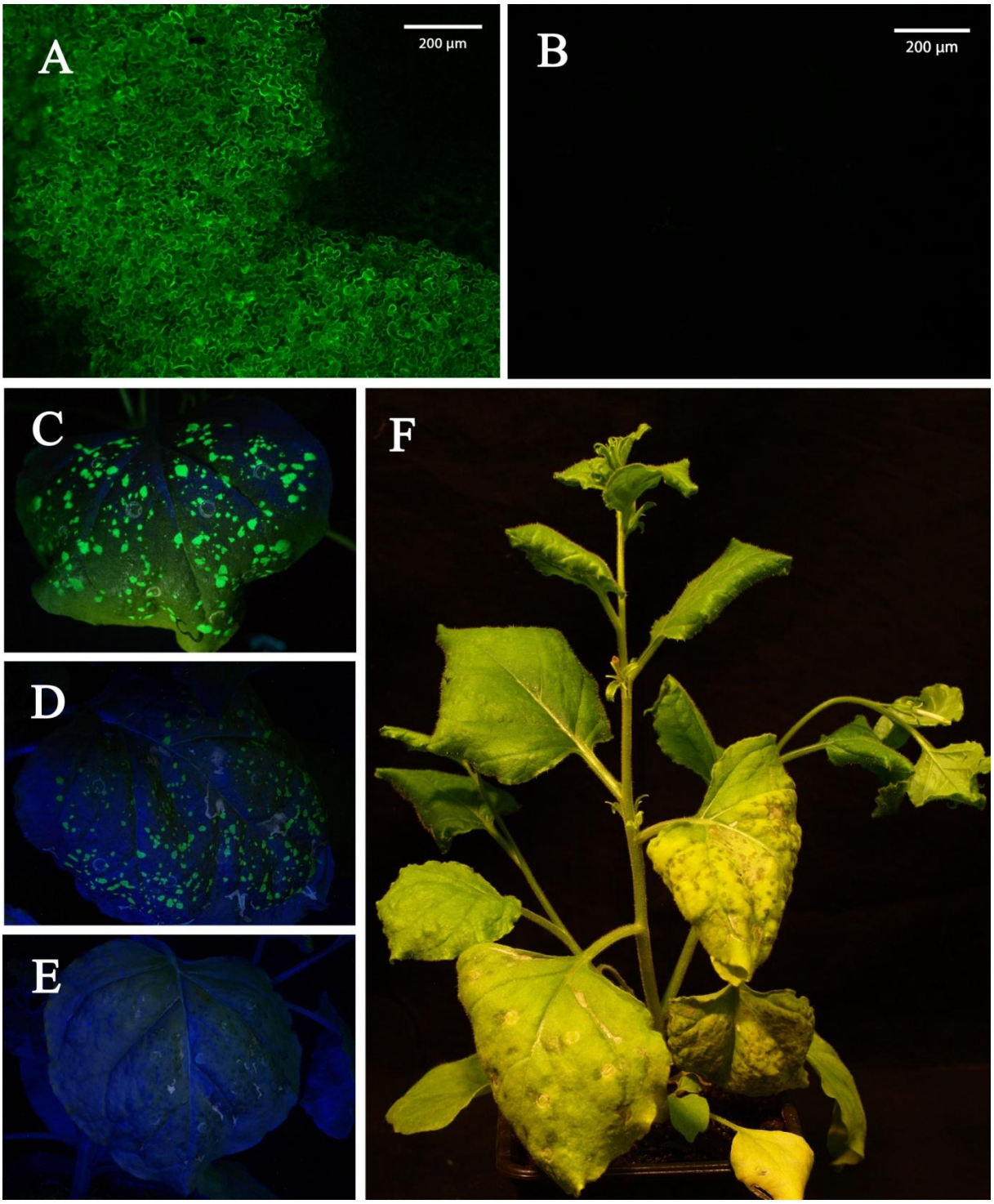

Figure 14: Symptoms on plants coinoculated with dRNA constructs and "helper" pGR2i-dCP construct. (A) The region of transformed cells on leaves agroinfiltrated with dRNA 3 and pGR2i-dCP constructs with GFP signal. **(B)** A negative control: cells agroinfiltrated only with "helper" pGR2i-dCP construct. Fluorescent signals on pictures A and B were visualized by fluorescence microscopy. **(C)** A leaf agroinfiltrated with dRNA 3 and pGR2i-dCP. **(D)** A leaf agroinfiltrated with dRNA 5 and pGR2i-TMV-dCP. **(E)** A leaf agroinfiltrated with dRNA 4 and pGR2i-dCP. Pictures A – E were photographed at 7 dpi. **(F)** K7 plant with symptoms after pGR2i-dCP agroinfiltrations, at 10 dpi. Leaves at the infected plant show typical symptoms of TMV on *N. bentamiana*.

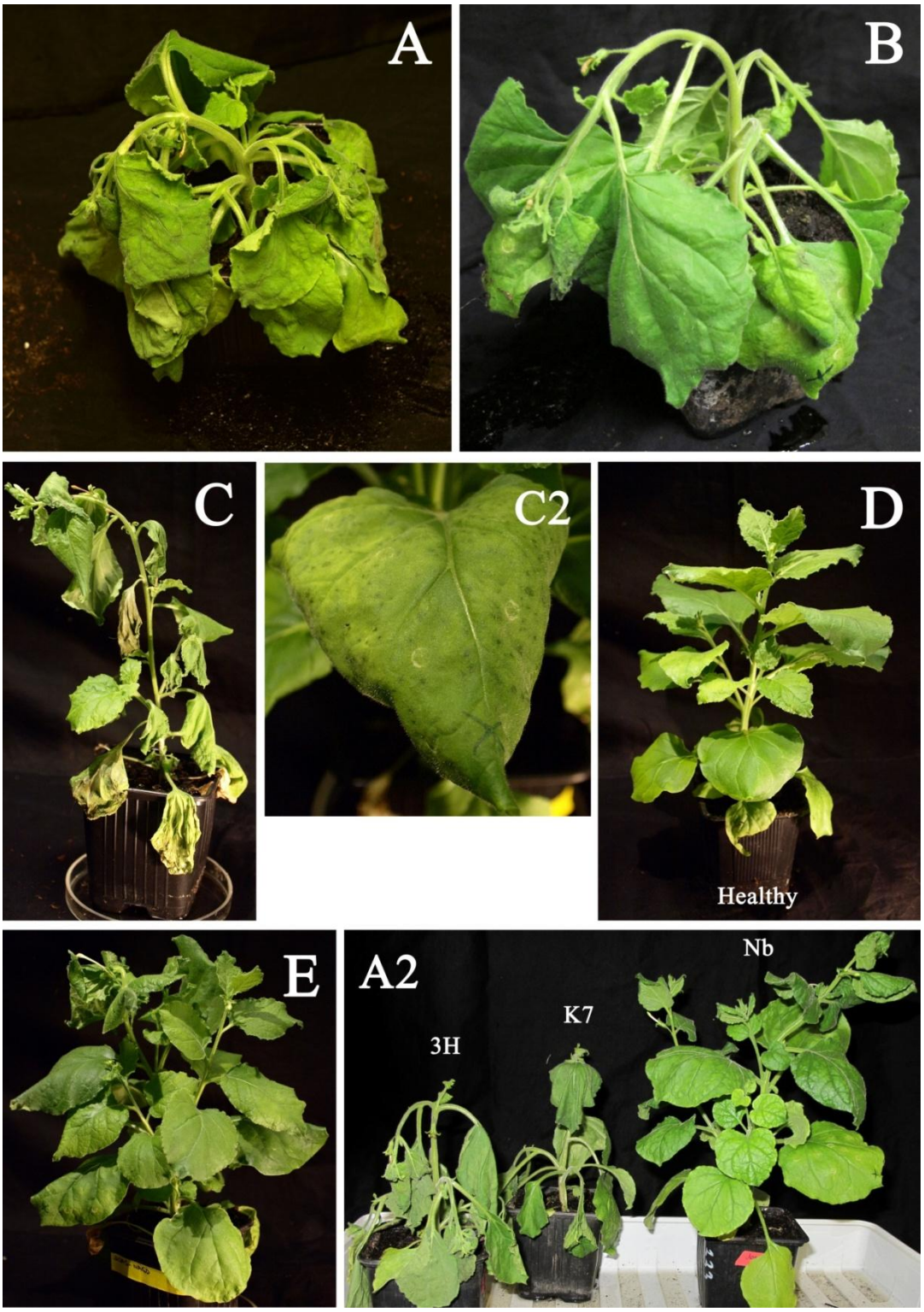

Figure 15: Symptoms on plants inoculated with helper constructs. (A) A wilted young K7 plant agroinfiltrated with the pGR2i-dOAS construct. (A2) Symptom comparison among plants of different genotypes. All plants were agroinfiltrated with pGR2i-dOAS. **(B)** A wilted young 3H plant agroinfiltrated with pGR2i-dOAS. **(C)** Nb plant agroinfiltrated with pGR2i-NAGD/CASP at 33 °C. **(C2)** A detail of symptoms caused by pGR2i-NAGD/CASP in Nb plant. **(D)** A non-infected control 3H plant. **(E)** 3H plant agroinfiltrated with pGR2i-dOAS-NAGD/CASP. Plants were photographed at 7 dpi. Young upper leaves of Nb plant (A2) and 3H plant (E) were deformed due to the lack of space in the growing incubator. Symptoms of TMV-U1 infection are very similar to or worse than the TMV-NAGD/CASP symptoms.

Infectivity of the extracts from plants agroinfiltrated with the helper constructs was tested using the hypersensitive response on Nt-NN plants. Infectious TMV particles present in these extracts produce local lesions on Nt-NN leaves. Local lesions were observed on plants inoculated with a pGR2i-NAGD/CASP extract and control purified TMV-U1. As expected, no lesions were found after infection with the extracts containing viruses without functional MP, since these viruses are not able to infect Nt-NN plants, the transgenic Nt-NN plants expressing MP would be required. We tested plant extracts infectivity on MP transgenic plants (3H and K7) and studied symptoms presence in the second step. Symptoms were observed in plants infected with TMV-NAGD/CASP, TMV-dOAS and TMV-dOAS2 extracts, but not in plants infected with TMV-dOAS-NAGD/CASP and TMV-dOAS2-NAGD/CASP. It should be noted that constructs TMV-dOAS-NAGD/CASP and TMV-dOAS2-NAGD/CASP did not produce visible symptoms even on 3H/K7 plants inoculated by agroinfiltration.

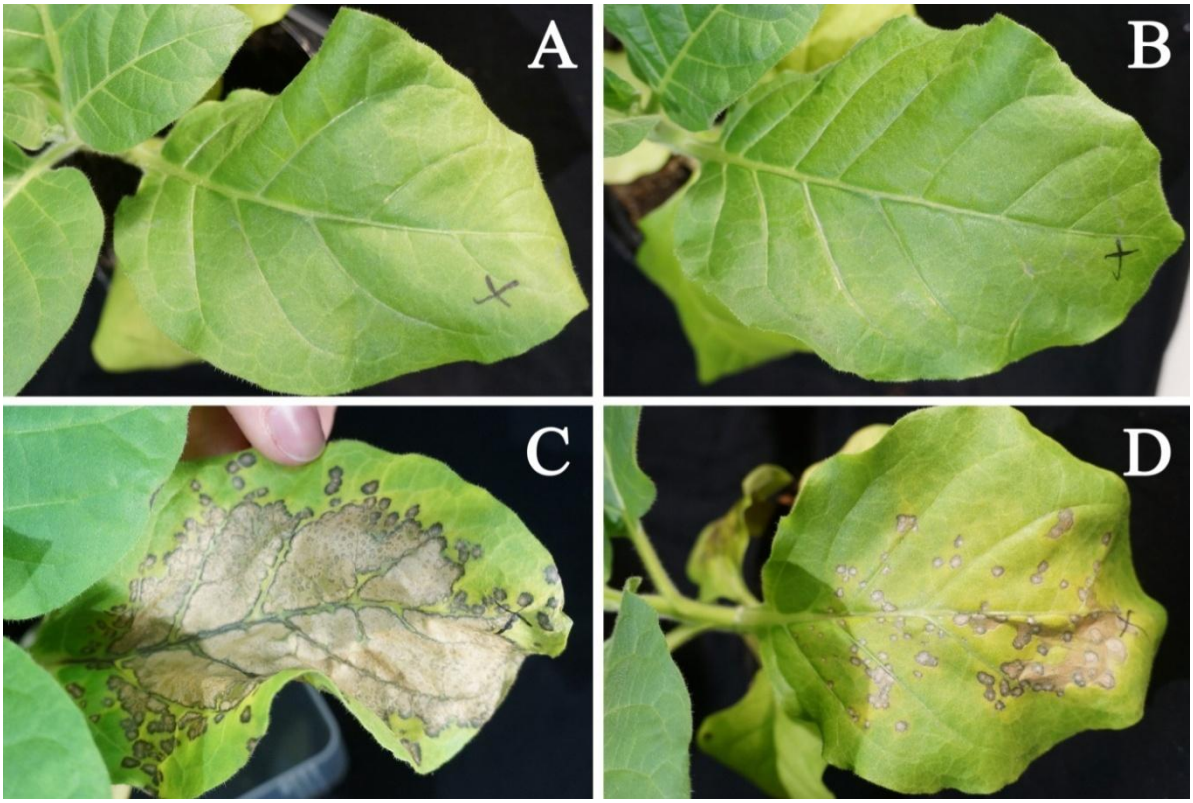

Figure 16: Hepersensitive response on Nt-NN plants at 5 dpi. (A) A plant infected with TMV-dOAS particles. **(B)** A plant infected with TMV-dOAS2 particles. **(C)** A plant infected with TMV-NAGD/CASP particles. **(D)** A plant infected with TMV-U1 particles.

Plant coinoculations by a mixture of two constructs followed after the initial tests of viability of individual constructs. Plants 3H and K7 were chosen for coinoculation. After 7 – 10 dpi the symptoms mostly corresponded to the symptoms of the helper virus that was contained in

the mixture. None of the coinoculated plants expressed GFP at a visible level or the GFP signal was too low to be detected. Additional details are shown in the following table:

Helper construct	dRNA construct	Plant symptoms	GFP signal
pGR2i-dOAS	dRNA 5	+	No
pGR2i-dOAS2	dRNA 1, 2, 3, 4, 5	++	No
pGR2i-NAGD/CASP	dRNA 5	+++	No
pGR2i-dOAS-NAGD/CASP	dRNA 5	?	No
pGR2i-dOAS2-NAGD/CASP	dRNA 1, 2, 3, 4, 5	?	No
pGR2i-TMV-dCP	dRNA 1, 2, 4	+++	No
	dRNA 3	+++	Yes
	dRNA 5	+++	Yes
-	dRNA 1, 2, 3, 4, 5	-	No

Table 4: Used combinations of the helper and dRNA constructs for agroinfiltration and its characteristics.

4.3. Detection of viral CP

The presence and quantity of the viral coat protein (17.5 kDa) in plant extracts was detected by a protein electrophoretic separation (SDS-PAGE) and immunodetection (Western blot) with anti-TMV antibodies. The immunodetection was performed to confirm the results and because it has higher sensitivity. The amount of the plant extract sample in Western blot was chosen according to the SDS-PAGE results.

A viral coat protein was detected in inoculated leaves of all helper constructs. The CP level was the highest in pGR2i-NAGD/CASP, then pGR2i-dOAS2 and pGR2i-dOAS. Helper constructs pGR2i-dOAS-NAGD/CASP and pGR2i-dOAS2-NAGD/CASP induced CP expression only in inoculated leaves and at very low level. The CP expression by pGR2i-NAGD/CASP was constant in the inoculated and even in the upper non-inoculated young leaves regardless of temperature. Helper constructs pGR2i-dOAS and pGR2i-dOAS2 caused several times higher CP accumulation in upper non-inoculated leaves in comparison to the inoculated leaves, but failed at the temperature of 33 °C. We have encountered a similar problem with constructs pGR2i-dOAS-NAGD/CASP and pGR2i-dOAS2-NAGD/CASP. The CP expression of all helper constructs was unchanged after coinoculation with the dRNA constructs, and the viral protein expression level was adequate to each helper construct.

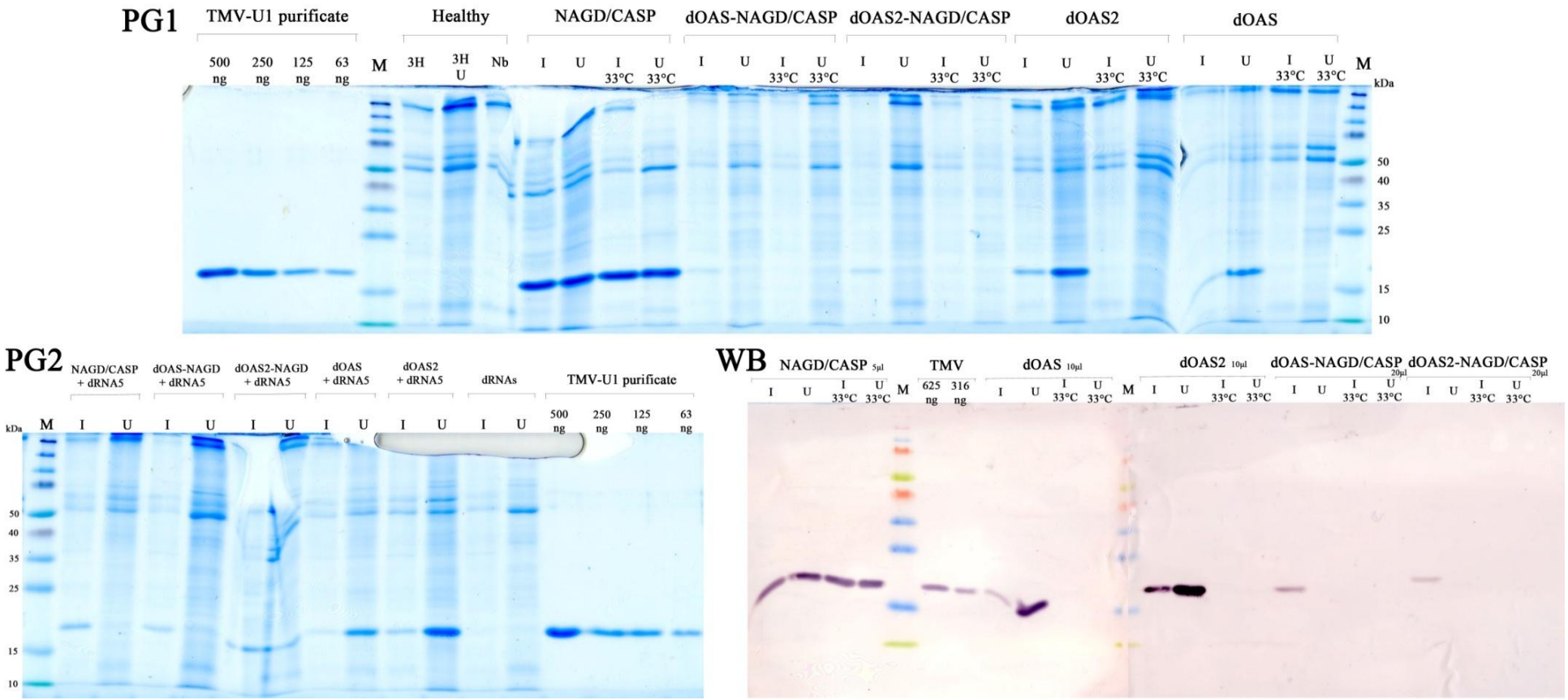

Figure 17: Stained polyacrylamide gels (PG1 and PG2) and Western blot immunodetection (WB). (I) – extract from inoculated leaves, (U) – extract from young upper non-inoculated leaves, (I 33°C) – extract from inoculated leaves at the temperature of 33 °C, (U 33°C) - extract from young upper non-inoculated leaves at the temperature of 33 °C. Volumes of extract used for immunoblot are indicated.

4.4. Analysis of RNA encapsidated in particles

Extracts from coinoculated plants (see Table 4) have also been used for a total RNA isolation followed by a reverse transcription to cDNA. Subsequently a series of PCR reactions was performed to detect GFP or CP sequence in cDNA.

The assumption was that all RNA unprotected by a viral capsid was degraded by RNases in chosen plant extracts after prolonged manipulation during extraction and analysis and only encapsidated RNA was isolated. Ten reverse-transcribed samples of cDNA (see Table 4) and one more sample containing a combination of TMV-NAGD/CASP with dRNA 5 at the temperature of 33 °C were used as templates for PCR reactions. As a positive control the GFP virus-like particles[1] (VLP; provided by T. Moravec) and an extract from the plant infected with wt TMV-U1 were included to confirm that both the RNA isolation and the reverse transcription were carried out in order. Appropriate plasmids served as positive controls.

The first set of PCR reactions (PCR-CP 1) with the primers qCP1 F and qCP1 R was performed to detect the CP sequence and to subsequently confirm the presence of the helper particles in the samples (except samples 1 – GFP-VLP, 3 – dRNAs and 15 – H_2O). The amplified sequence should have the length of 169 bp and it was detected in all samples. It was also confirmed in all positive and negative controls. The second CP sequence detecting set of PCR reactions (PCR-CP 2) was made with the primers TMV-sgCP F and TMV-3´NTR R. These primers should amplify fragment of different lengths depending on the template – about 760 bp for the helper cDNAs and about 1050 bp for GFP VLP cDNA and cDNAs from dRNA 3 and 5. The resulting fragments conformed to the expectations. Control PCR-CP 2 set was performed with RNA isolated from samples as the template and under the same conditions as PCR-CP 2. This Control PCR-CP 2 should determine the level of DNA contamination in the RNA samples. The fragments of different length were the result but the quantity of fragments compared to the positive control fragment was very weak (see Figure 18).

Simultaneously, the set of PCR reactions detecting the GFP sequence was done in order to determine whether the coat protein expressed by the helper virus has the affinity to package target dRNAs. The first reaction set PCR-GFP 1 used primers qGFP F and qGFP R and

[1] These particles were formed after the plant agroinfiltration with the constructs pGR2i-dCP-GFP and PVX virus expressing the TMV coat protein. The GFP-VLP were then purified by sucrose cushion centrifugation.

amplified fragment length of 247 bp. A positive signal was detected using both positive controls (sample 14 - plasmid positive control and sample 1 – GFP VLP) but also by sample 12 (TMV-dOAS2 + dRNA 3) and sample 13 (TMV-dOAS2 + dRNA 1, 2, 4). To confirm these results, the PCR-GFP 2 set was done also with primers GFP2 F and P2 R. These primers amplify longer 616 bp fragment exclusively from dRNAs cDNA template (they do not interact with GFP-VLP cDNA). The results from this PCR set confirmed the results from PCR-GFP 1 set, although the positive signal of sample 12 was much weaker.

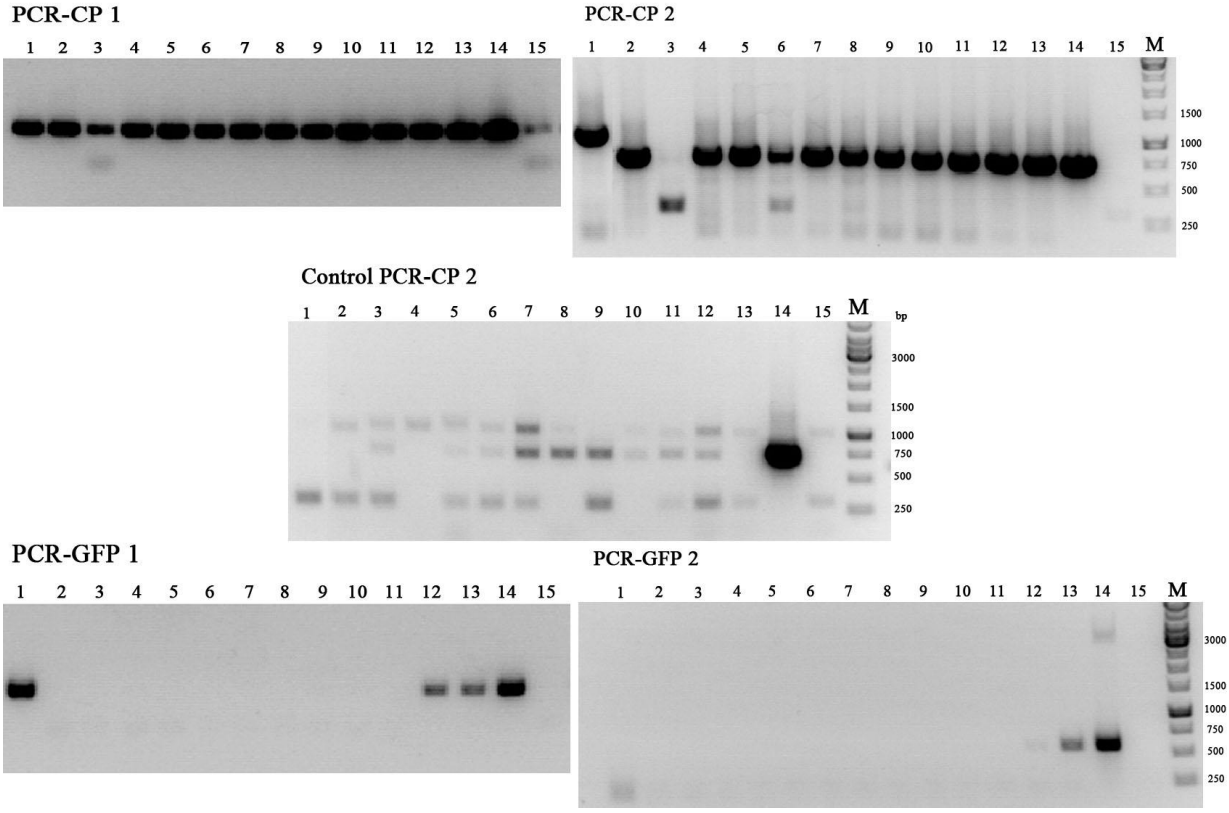

Figure 18: Amplified DNA fragments after PCR from cDNAs / RNA template. cDNA samples were used as template for PCR-CP 1 and 2 and PCR-GFP 1 and 2 reactions, while isolated RNA samples were used as template for control PCR-CP 2 reactions in order to detect DNA contamination in samples. **(1)** GFP VLP (10x diluted) as the positive control for PCR-GFP reactions. **(2)** TMV-U1 as the positive control for PCR-CP reaction. **(3)** dRNAs – as the negative control for all PCR reactions. **(4)** TMV-NAGD/CASP + dRNA 5. **(5)** TMV-NAGD/CASP + dRNA 5 at 33 °C temperature. **(6)** TMV-dOAS-NAGD/CASP + dRNA 5. **(7)** TMV-dOAS2-NAGD/CASP + dRNA 5. **(8)** TMV-dOAS2-NAGD/CASP + dRNA 3. **(9)** TMV-dOAS2-NAGD/CASP + dRNA 1, 2, 4. **(10)** TMV-dOAS + dRNA 5. **(11)** TMV-dOAS2 + dRNA 5. **(12)** TMV-dOAS2 + dRNA 3. **(13)** TMV-dOAS2 + dRNA 1, 2, 4. **(14)** Plasmid positive control for each appropriate PCR reaction. Plasmid pGR2i-dOAS for PCR-CP reactions and plasmid pGR2-GFP for PCR-GFP reactions were used as template. **(15)** Non template control – H_2O. **(M)** Marker GeneRuler 1 kb DNA Ladder. Unfortunately the marker for PCR-CP 1 and PCR-GFP 1 samples is missing but the positive controls are present.

4.5. Particle visualization and measurement

In order to provide evidence of viral particles in inoculated plants the visualization by a transmission electron microscope was necessary. Particles were detected in all extracts from the plants inoculated with helper viruses (see Figure 19) and even in extracts from plants coinoculated with combination of helper and dRNA contructs that were identified as positive in PCR test (see Figure 18, combinations TMV-dOAS2 + dRNA 3 and TMV-dOAS2 + dRNA 1, 2, 4). The particles in each chosen sample were measured by iTEM programme in order to determine the most common particle length in plants. The obtained data were further arranged in histograms showing the percentage of the particles of given length.

The most abundant particle length of control TMV-U1 particles was 240 – 270 nm. Two more minority peaks were observed at 50 – 60 nm and 80 – 90 nm. Compared to TMV-U1, the TMV-NAGD/CASP distribution of the particles was shifted mainly to short particles. The most abundant particle size was 30 – 60 nm. Particles TMV-dOAS and TMV-dOAS2 showed a clear peak at 250 – 260 nm and smaller particles were represented only in small quantities. Measurement of the particle size distribution of TMV-dOAS2-NAGD/CASP and especially of TMV-dOAS-NAGD/CASP was more difficult due to the very low number of particles in the extracts. The obtained data are therefore less convincing, because they were based on the three times and eight times fewer particle numbers than for other helper viruses. We can assume that the TMV-dOAS2-NAGD/CASP particle size distribution is shifted to the shorter particles as well as the TMV-NAGD/CASP but the main peak is 80 – 100 nm (see Chart 1).

The particle size distribution of combinations of TMV-dOAS2 + dRNA 3 and TMV-dOAS2 + dRNA 1, 2, 4 broadly followed the distribution of the helper virus TMV-dOAS2, but there was a significant growth of the number of shorter particles in the range 50 – 180 nm (see Chart 2). The particle size distribution of the combination TMV-dOAS2 + dRNA 5 was made as well because, initially, we thought that the dRNA 5 will be most abundant and thus its encapsidation most easy to spot. There was, however, no significant increase of short particles distribution contrary to the two GFP positive samples in PCR.

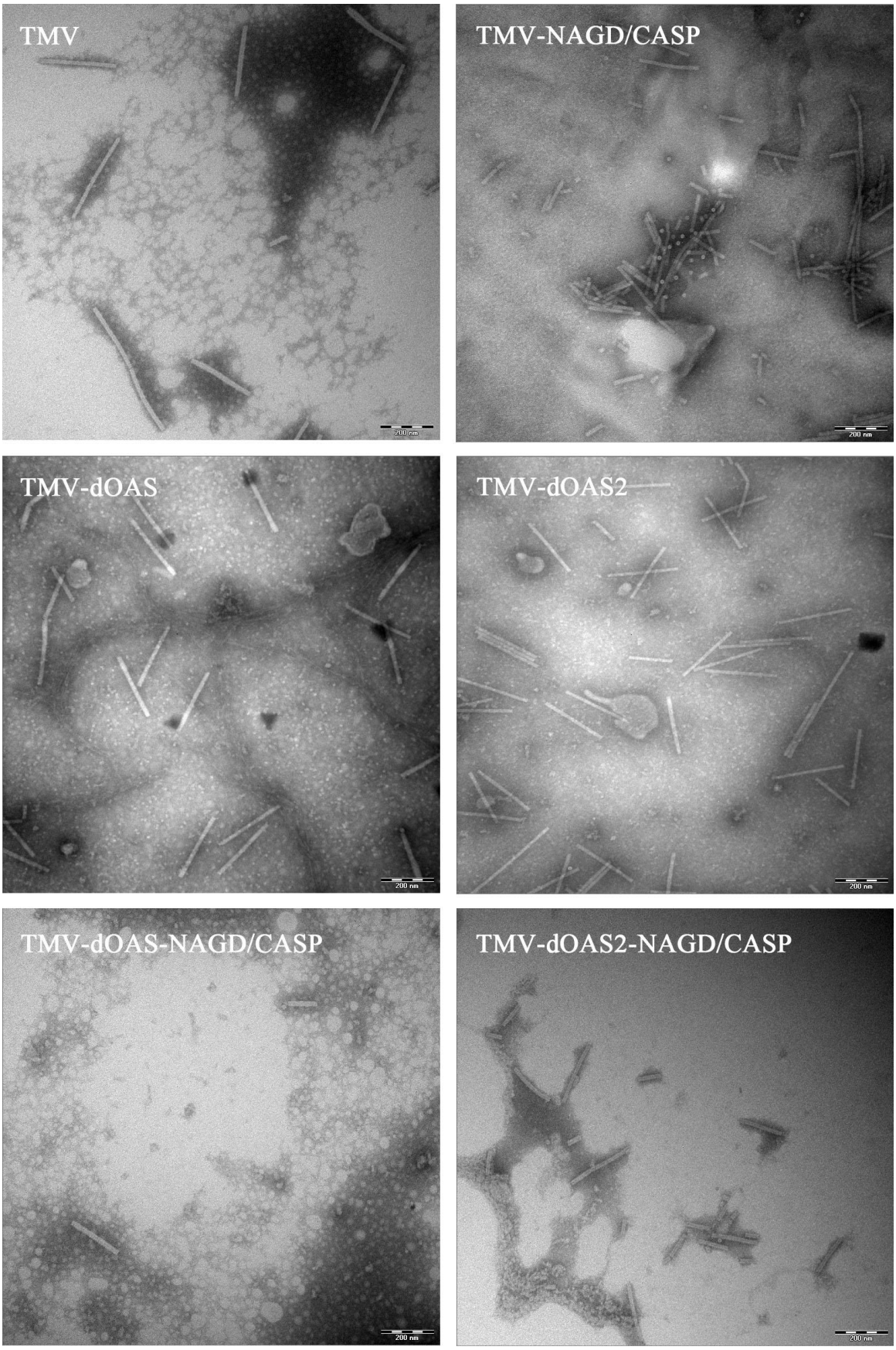

Figure 19: Negatively stained viral particles visualized by transmission electron microscope. Scale bar represents 200 nm.

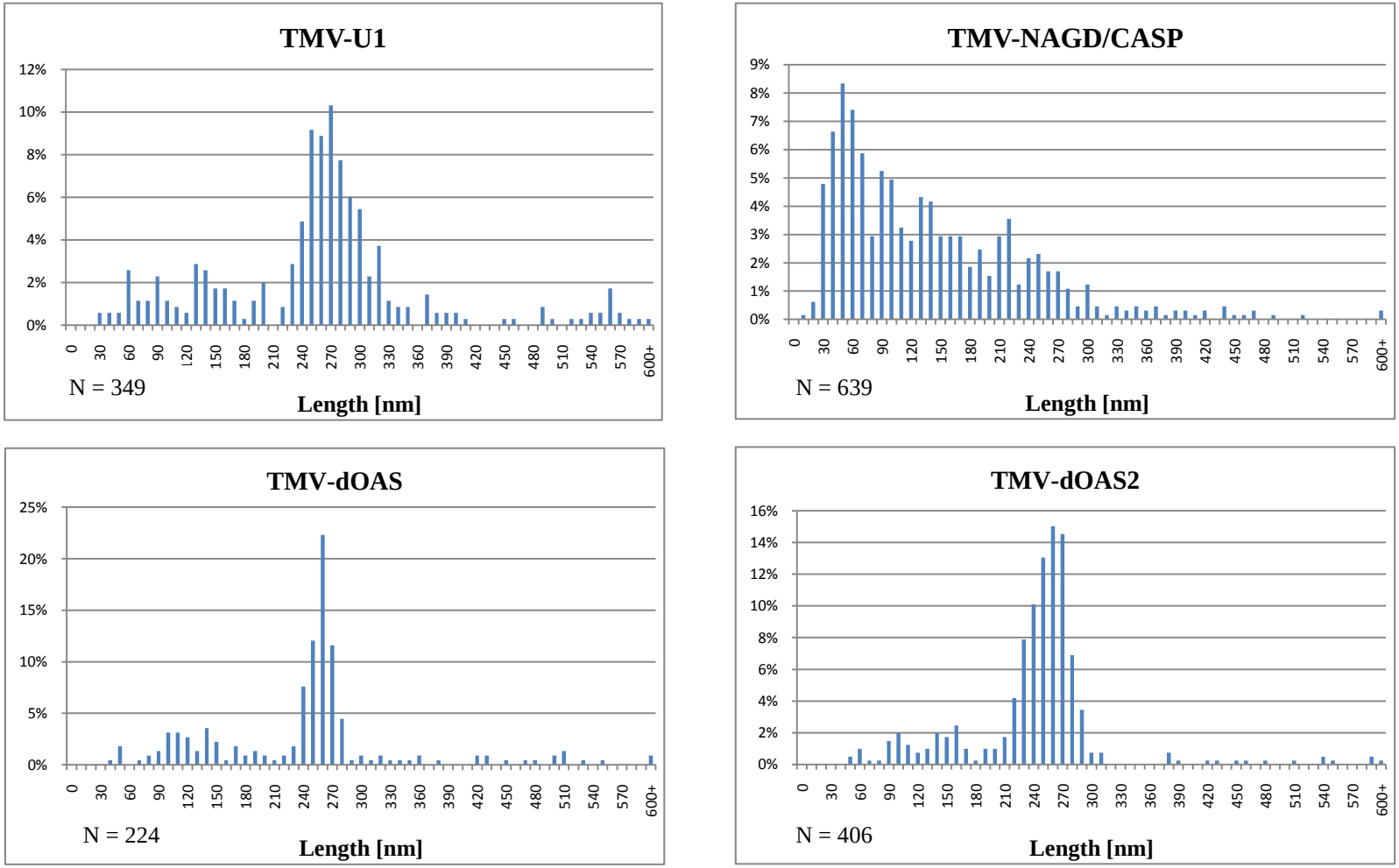

Chart set 1: Representation of the particle length distribution for each helper virus. N – number of measured particles.

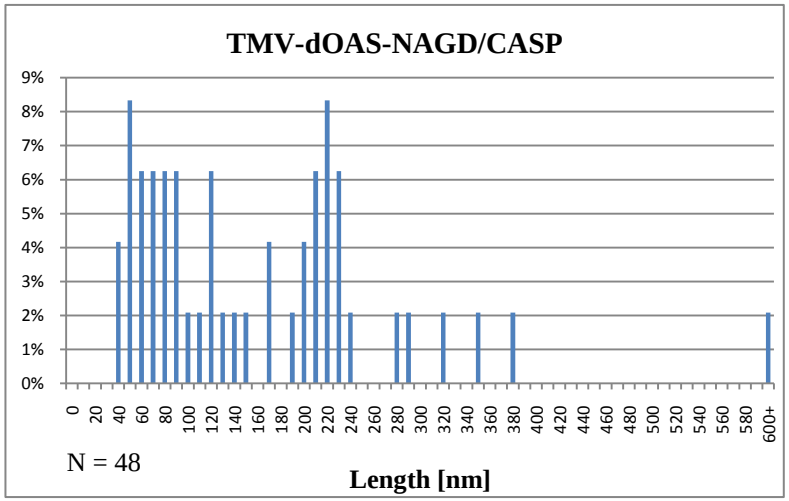

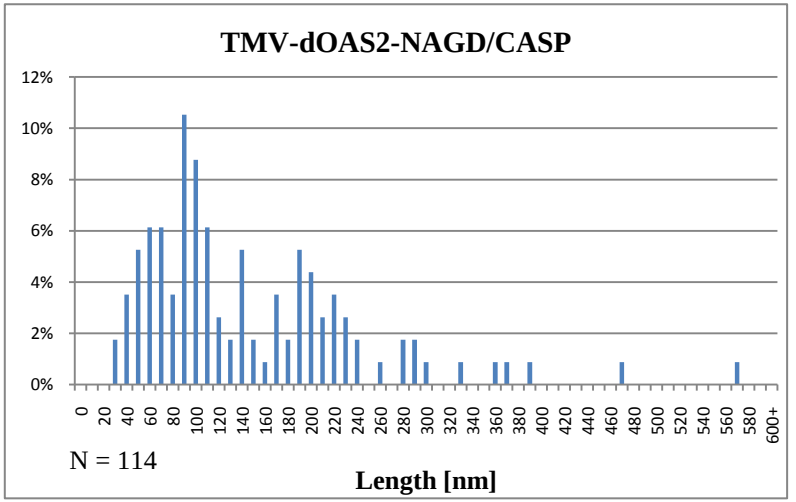

Chart set 2: Representation of the particle length distribution for each helper virus. N – number of measured particles.

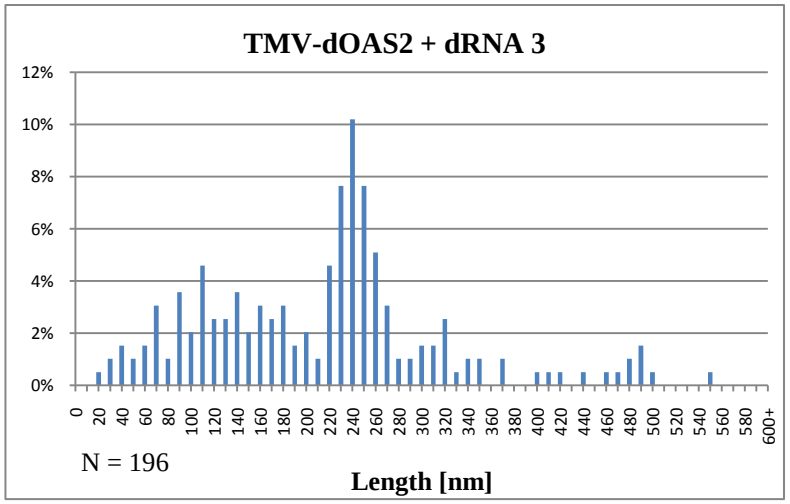

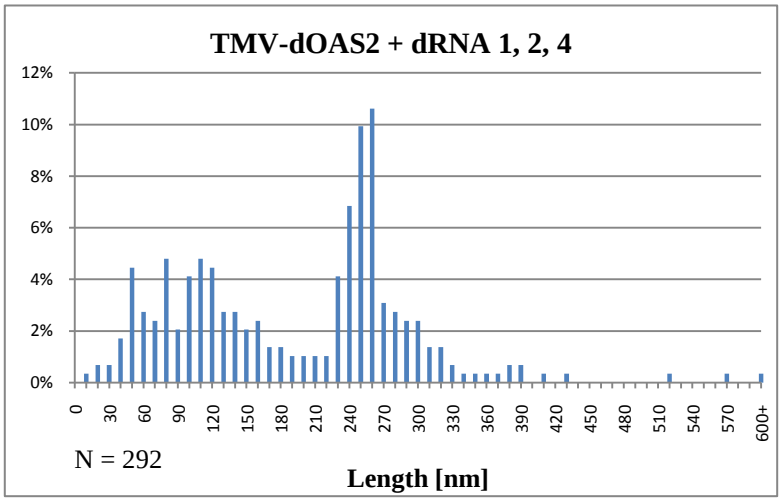

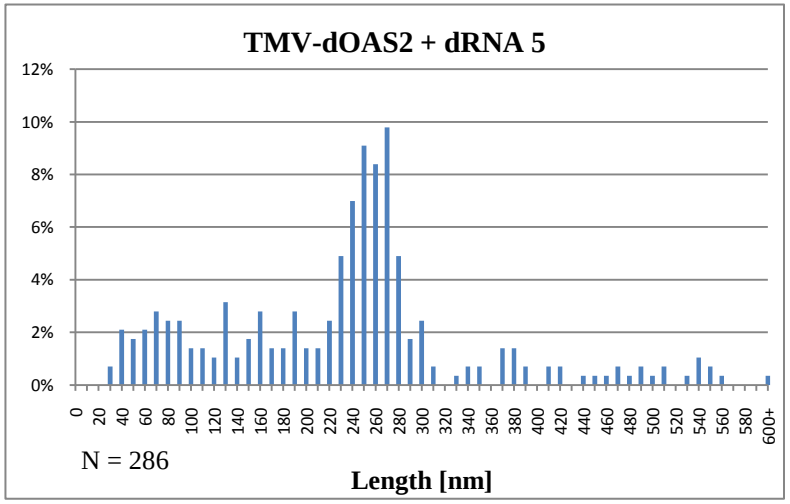

Chart set 3: Representation of the particle length distribution for GFP positive samples. N – number of measured particles.

5. DISCUSSION

The main aim of this work was the *in planta* production of TMV particles with specified length. For this purpose, the work was divided into several parallel goals that are closely connected to each other.

5.1. Construction of satellite dRNAs designed for effective and quantitative packaging of particles

First part of the work merged first two goals and was focused on the design of a satellite RNA with minimal set of features necessary for its replication and encapsidation by TMV CP. For easy detection the GFP sequence was included in the proposed dRNAs and flanking sequences were designed for easy GFP replacement. The dRNA should then be replicated with the help of viral RdRp and encapsidated by TMV-CP in cells with parallel replication of helper virus. Our constructed dRNAs varied in the length of the remaining TMV RdRp sequence and in the presence or absence of the subgenomic CP promoter. RdRp sequence fragments of different lengths (none, first 378 and first 778 bases from the start codon) were included in the dRNAs because it was assumed that they could comprise *cis*-acting regions necessary or enhancing dRNA replication. This design was similar to the design described in Roy et al. (2010) who proposed two-component TMV-based system for high-level expression of multiple proteins in plants. The dRNA constructs described by Roy and others contain first 773 nucleotides of TMV RdRp sequence as well as the sgCP promoter and considerable part of 3'end of TMV RNA starting within the MP coding region (from position 5182 of genomic RNA). The described construct allowed achieving of high expression level of reporter or therapeutic proteins under the sgCP promoter.

The dRNA replication in infected cells could be detected using GFP signal. The GFP signal was detected only in the plants infected with dRNAs containing sgCP promoter (dRNA 3 and dRNA 5) in the presence of a helper virus without its own CP (see 4.2). When the used helper virus contained CP, the GFP signal disappeared even when sgCP containing dRNAs (dRNA 3 or 5) were used. We assume that it was caused by preferential CP packaging of the transcribed sgGFP RNA containing the encapsidation signal (OAS_{75}), which competed with its translation. The GFP intensity was similar in both dRNA 3 and dRNA 5 constructs. We have found, that the minimal length of the RdRp sequence for dRNA parallel replication with the helper virus, can be about 400 bases shorter than was described by Roy et al. (2010). Moreover, the dRNA constructs designed by Roy contained original TMV sequence from

the 5182 position to the 3'end. Our constructs contained in this region only 3'NTR and sgCP promoter sequences and were replicapable. The sgCP promoter seems to be a necessary condition for practical use. In constructs without sgCP promoter (for example dRNA 2 and 4 which are analogous to dRNA 3 and 5) we have conflicting results regarding their ability to be recognised by viral replicase, however it is clear that their accumulation levels are too low for reliable detection of GFP fluorescence and also for practical use.

5.2. Elimination of the encapsidation signal does not change the coat protein specificity to the viral RNA

The second part of this work was to remove encapsidation signal / origin of assembly (OAS) from viral sequence to prevent helper virus packaging (goal 3). Our first helper construct had most of the MP ORF from the viral genome removed. Only a short central part (with 23 bases from core OAS_{75}) and the last 161 bases of MP ORF (containing minimal sgCP promoter) were preserved (see Figure 11). This construct successfully infected transgenic plants and showed similar symptoms as wt TMV and also the accumulation of CP was similar to wt TMV as shown by SDS-PAGE and immunoblot analysis. However, images from electron microscope surprisingly demonstrated the presence of large numbers of full-length virus particles (TMV-dOAS) in the plant extract. The second helper construct was therefore prepared with deletion of 61 additional bases from central part of the MP ORF (see Figure **11**). This second helper virus showed even a little higher aggressiveness in plants and, surprisingly, produced large numbers of TMV-dOAS2 particles (see Figure 19). Infectivity and symptoms of this construct were otherwise similar to the first helper construct. Thus the removal of core OAS as has been described by Turner & Butler (1986) and which is necessary for assembly *in vitro* does not have an impact on particle assembly *in vivo*.

The unexpected results imply that the deletion of neither the OAS_{75} sequence nor most of MP sequence does not change coat protein ability to specifically recognize viral RNA and to assemble particles *in planta*. The work of the authors Turner & Butler (1986) established loop 1 (OAS_{75}) as the key area for rapid and efficient packaging of even foreign RNA sequence by TMV coat protein disks. They characterized the sequence AAGAAGUCG (apex of the stem-loop 1 structure) which is instrumental in disk binding and assembly initiation and they further determined that the guanine regular repetition is the principal sequence feature for binding. However, the experiments performed in the work from 1986 were performed *in vitro* and their approach was substantially different from this work, which

relies on *in planta* system. Turner and Butler performed an assay for the nucleation of TMV assembly disks and RNA transcribed *in vitro*. To dissect the functionally important parts of the TMV assembly origin, they altered and deleted parts of OAS sequence and then measured the effect on RNA encapsidation by disks. The authors themselves admit that throughout the whole viral process the sequences may contain another minority encapsidation signals. We assume that such a minority signal could be located within the replicase ORF. This theory is even supported by the fact that the *in vitro* packaging of coat protein transcript failed similarly to other unsuccessful transcripts (Turner & Butler, 1986). To localize these minor encapsidation signal(s), it would be necessary to clone further constructs with replicase protein function retained, but with altered codon bias.

Even though the helper virus retained its encapsidation competence, we have proposed that the stability of RNA/CP complexes might be compromised by OAS removal, and that at a higher temperature we might be able to reach our goal to prevent CP from packaging the helper virus genomic RNA. We have proposed that the higher temperature might alter RNA structure which could then result in elimination of the functions of hypothetical minor encapsidation signal(s) and favour packaging of the target dRNA with complete OAS_{75} by CP disks. Surprisingly there was no detectable CP expression at elevated temperature in plants inoculated with dOAS/dOAS2 helper viruses, while viruses containing OAS replicated normally. One of the possible explanations might be the proximity of sgCP promoter to the removed OAS/MP sequences which might affects activity of this promoter. From the available data it is difficult to differentiate between non-replicating helper virus and helper virus that does not produce CP; however, based on the absence of symptoms we assume that the dOAS/dOAS2 helper viruses were replication incompetent at elevated temperature.

The particle length measurement of TMV-dOAS and TMV-dOAS2 revealed an interesting additional feature of these helper viruses. The calculated length of full particles with deletions in the RNA sequences was about 274 nm for TMV-dOAS and 271 nm for TMV-dOAS2 (see Table 2). The length of wt TMV-U1 particle is known to be around 300 nm. However, the viruses TMV-U1, TMV-dOAS and TMV-dOAS2 had the highest proportion of particles of about the same length 270 nm which corresponds to the calculated lengths for dOAS/dOAS2 helper viruses but not for TMV-U1. We cannot explain this result but only speculate that this was caused by homogenization method, which could contribute to the particle breaking. We would, however, expect that the breaking would create shorter particles, since the mechanical breaking of particles is most likely to occur around the central

part of the particle. The particle length distribution in the charts may also be distorted by the rod-shaped particles tendency to aggregate and concatenate in a row.

Future experiments might be directed towards identification and removal of minor OAS from TMV sequence and/or on separation of large full-length particles from the encapsidated dRNA. It might also be possible to use a third unrelated helper virus to provide the CP protein.

5.3. Modified CP-NAGD/CASP is able to form particles but without specificity to the viral RNA

The third part of this work was focused on the TMV coat protein modification in the inner channel area in such a way that a metal-binding peptide would be inserted while all attributes necessary for the binding of viral RNA and particle formation would be retained (goal 4). We have chosen the peptide NAGDHAN with the ability to bind Co and Pt metals (Mao et al., 2004). Such modified particle should bind metals specifically within the central channel after metallization, for example, by electroless deposition (Balci et al., 2006). The resulting metal nanoparticles would have controllable ratio of length and width and specific metal would be stored in a biocompatible protein shell which can be further modified in multiple ways such as by binding variable ligands. Such particles would have an interesting application potential in both basic research and in the diagnosis and treatment of human diseases.

Selection of an appropriate site for the target peptide insertion is based on the known 3D structure of TMV-CP (Namba et al., 1989). Since the inner channel loop is not clearly visible on the X-ray structure images, it was suggested that it forms undefined coiled-coil structure and thus it may be modified without disruption of particle formation. Previous modifications of this region that was performed by T. Moravec only inserted peptide into target site with no other mutations in the CP sequence. The result of this modification was named CP-NAGD. However, this CP was able to form short particles but its infectivity was completely abolished. Since the distribution of positive and negative charges strongly affects the particle stability (Wang et al., 1998), additional mutations near peptide insertion region have been made to create CP-NAGD/CASP protein (Moravec, unpublished). The charge in the central channel was therefore adjusted to resemble the natural state. These additional "CASP" mutations replaced glutamates at the position 97 and 99 with negative charge (so-called Caspar carboxylates; Caspar, 1964) by glutamines with neutral charge. The assumption was that the insertion of metal-binding peptide NAGDHAN should not affect

the coat protein RNA-binding affinity because the RNA does not have any direct contact with the amino acids forming the inner channel.

Our construct containing a viral full-length cDNA clone with modified CP was able to infect plants using agroinfiltration, cause typical symptoms in inoculated plants, produce CP-NAGD/CASP at a level comparable to the wt TMV. Moreover it was replication/assembly competent at elevated temperature of 33°C and the extract from infected plants retained infectivity. All these results pointed to conclusion, that compensation mutations "CASP" have restored particle formation. However, particle length measurement after electron microscopy demonstrated that the particle distribution was strongly biased towards shorter particles (see TMV-NAGD/CASP in Chart set 1). This result implies that the CP-NAGD/CASP specificity for viral RNA was largely or completely lost and this modified coat protein is not able to efficiently recognize encapsidation signal. Alternatively this can be explained by high fragility of TMV-NAGD/CASP particles, however partially disassembled particles of unstable mutants that can usually be observed on EM grids were not seen it this case. Another possibility is that CP-NAGD/CASP preferentially forms empty virus-like particles (VLP) without encapsidated RNA. This corresponds to particle length measurement of plant extracts inoculated with a full-length cDNA clone of Potato Virus X where the original coat protein was replaced by CP from the wt TMV. The particle distribution in such plant extracts was very similar to the TMV-NAGD/CASP (data are not shown). One possible way to determine whether particles contain RNA is particle purification followed by gradient centrifugation. Individual fractions would be examined by UV spectroscopy where the absorption spectrum should indicate whether RNA is present, and "full" particles from VLPs would be separated and quantified. We expect that similar results would also be provided by PCR after RNA isolation and reverse transcription from individual fractions. These experiments however were beyond the scope of this thesis, but we plan to perform them in the near future as well as the particle metallization. Also infectivity test of individual fractions on hypersensitive plant host might be used to differentiate between empty VLPs and virus particles.

5.4. TMV based two-component system for the production of specific-length particles in plants

The last part of this work connects all the previous parts together and achieves the final goal of the thesis which is an attempt to find a system for the *in planta* production of viral particles with specific-length (goal 5). Ideally, we would like to produce particles of uniform length and with modification in the inner channel for the potential metallization. Particles should be obtained by combination of two constructs. dRNA construct provides dRNA for particle assembly and a helper construct provides (modified) coat protein for packaging and RdRp for replication of both dRNA and helper RNA. The simultaneous infection of cell by both constructs is therefore necessary because the dRNA replication is dependent on the replication of the helper virus. Ideally, the helper viruses would not contain encapsidation signal (OAS) to avoid incorrect-length particle assembly. The dRNA contains only 5'NTR and 3'NTR terminal viral sequences required for recognition by viral RdRp and the viral OAS sequence necessary for specific recognition by coat protein and thus for particle assembly. The dRNA also contains reporter sequence (GFP) for easy detection. The dRNA length determines the length of the resulting particles.

Constructs producing TMV-dOAS-NAGD/CASP and TMV-dOAS2-NAGD/CASP were prepared to create an ideal helper virus. These helper viruses do not contain OAS similarly to helper viruses TMV-dOAS and TMV-dOAS2 and additionally express modified CP-NAGD/CASP. The last helper virus TMV-NAGD/CASP was sequentially the most similar to the wt TMV-U1 – it contained the OAS, but CP had been modified. We compared the coat protein expression level of all helper viruses to find that TMV-dOAS-NAGD/CASP and TMV-dOAS2-NAGD/CASP levels were very low in comparison with remaining viruses (see Figure 17). The CP-NAGD/CASP of those two viruses was also not detected in the upper, non-inoculated leaves, so viruses apparently do not spread through the plant. This suggests an interesting interplay between the OAS and the CP modification and also that minor modifications of CP might be used to improve its specificity towards the correct OAS.

The constructed dRNAs varied in the length of the TMV RdRp sequence and in the presence of the subgenomic CP promoter. The selection of transgenic plant producing viral movement protein was necessary for most of coinoculations by both construct types. Because the OAS sequence exclusion from most of the helper viruses also disrupted the MP expression. In this work we have selected several combinations of dRNA and helper virus (see Table 4)

to reduce the experimental complexity. We expected dRNA 5 (with 778 bases from RdRp and sgCP promoter) to be the most promising dRNA for particle assembly, however the TEM observations along with RT-PCR analysis showed that similar RNA 3 showed higher proportion of dRNA containing particles.

The particles from the coinoculated plants were extracted and the RNA isolated and then transcribed to cDNA. cDNA samples were then used for PCR in order to detect a GFP sequence and thus the presence of the target dRNA in particles. Results showed dRNA presence only in particles from plants coinoculated with TMV-dOAS2 helper virus. The ability to be packed by CP was clearly demonstrated in dRNA 3. It was also demonstrated in the mixture of dRNA 1, dRNA 2 and dRNA 4. This is in agreement with the data obtained from TEM particle measurement.

Attempts to disrupt CP affinity to helper virus genomic RNA using higher temperature completely abolished the CP expression and possibly even RNA replication of viruses without OAS. Additional experiments with more extensive range of temperatures would shed more light on the mechanism of this phenomenon. Interestingly, the seemingly most straightforward goal on the path to *in planta* system for the production of uniform length particles of specific length proved most difficult. The removal of known and well described OAS did not affect the encapsidation potential of TMV genomic RNA, thus making the ultimate goal more difficult to achieve. It was suggested that the CP would preferentially bind to OAS located in dRNA. The majority of CP would then be bound in short particles containing dRNA Surprisingly, the plant extracts still contained majority of full-sized particles with a small but significant shift towards shorter species where dRNA was present. Based on the available data both dRNA 3 and dRNA 5 posse similar ability to form particles.

In this work we have attempted to combine several phenomena with a goal to create uniformly sized short TMV-based particles *in planta*. While some of these phenomena were well described in the literature (OAS by Turner and Butler, 1986; dRNA by Roy et al., 2010), the novelty of this work lies in the combination of several functional steps to provide qualitatively novel way to use rod-shaped plant virus. Also the ability to modify inner channel of TMV with a metal binding peptide, while retaining virus infectivity, is completely novel and not described in the scientific literature. Another contribution of this work is the improvement of the dRNA vectors, which were significantly reduced in size.

Helper construct	Symptoms	CP expression level	Particle presence	Ability to encapsidated dRNA	Infectivity
pGR2i-dOAS	Yes	+++++	Yes	No	Yes
pGR2i-dOAS2	Yes	++++++	Yes	Yes dRNA 3 dRNA 1 / 2 / 4	Yes
pGR2i-NAGD/CASP	Yes	++++++	Yes	No	Yes
pGR2i-dOAS-NAGD/CASP	No	+	Yes	No	?
pGR2i-dOAS2-NAGD/CASP	No	+	Yes	No	?

Table 5: Summary of the characteristics of helper viruses. The dRNA encapsidation ability was evaluated according to the PCR results.

6. SUMMARY

The constructs for production of satellite dRNA capable of parallel replication dependent on TMV RNA were designed and prepared. All constructs contained encapsidation signal sequence for particle assembly by TMV CP and a GFP reporter cassette which can be easily removed and replaced with another sequence of choice. The dRNA constructs varied by the length of the TMV RdRp sequence and by the presence or absence of the subgenomic CP promoter. The dRNA constructs containing a sgCP promoter allowed for high level expression of the inserted GFP gene in parallel with a helper virus. This ability, along with their small size, makes dRNAs a very useful vector system for the general protein or RNA expression in plants.

The encapsidation signal from TMV genome was removed in order to avoid RNA packaging. Surprisingly, both deletion variants were still able to form particles. It is possible that some other sequence motifs, still present in the genomic RNA, might contribute to the encapsidation specificity. We have also observed that at elevated temperature the OAS deletion leads to a complete abolition of the virus replication.

The construction of a full-length TMV cDNA construct with a modified coat protein in the protein inner channel region was performed. The modified coat protein is apparently able to form particles but with reduced specificity to viral RNA. Most of the particles observed by an electron microscopy were abnormally short and might have been empty, but at least a considerable fraction contained an infectious viral RNA, since the particles retained their infectivity.

In planta system for the production of defined length particles containing defined RNA with modified inner channel was designed and performed. Uniformity of the particle lengths was compromised by the ability of the helper virus to still form particles. We have showed that some proportion of particles contained our designed dRNA encapsidated with wt TMV CP; however, binding of modified coat protein to dRNA has not been demonstrated.

7. REFERENCES

Abel PP, Nelson RS, De B, Hoffmann N, Rogers SG, Fraley RT, Beachy RN. **1986**. Delay of disease development in transgenic plants that express the tobacco mosaic virus coat protein gene. *Science* **232**: 738–743.

Balci S, Bittner A, Hahn K, Scheu C, Knez M, Kadri A, Wege C, Jeske H, Kern K. **2006**. Copper nanowires within the central channel of tobacco mosaic virus particles. *Electrochimica acta* **51**: 6251–6257.

Balique F, Colson P, Barry AO, Nappez C, Ferretti A, Al Moussawi K, Ngounga T, Lepidi H, Ghigo E, Mege J-L, *et al.* 2013. Tobacco Mosaic Virus in the Lungs of Mice following Intra-Tracheal Inoculation. *PloS one* **8**: e54993.

Balique F, Colson P, Raoult D. **2012**. Tobacco mosaic virus in cigarettes and saliva of smokers. *Journal of Clinical Virology*.

Baulcombe DC. **1996**. Mechanisms of pathogen-derived resistance to viruses in transgenic plants. *The Plant Cell* **8**: 1833.

Beachy RN, Zaitlin M. **1977**. Characterization and in vitro translation of the RNAs from less-than-full-length, virus-related, nucleoprotein rods present in tobacco mosaic virus preparations. *Virology* **81**: 160–169.

Beijerinck M. **1889**. Über ein contagium vivum fluidum als Ursache der Fleckenkrankheit der Tabaksblätter. Kon. Akad. Wetensch. Amsterdam.3–21.

Butler P. **1999**. Self-assembly of tobacco mosaic virus: the role of an intermediate aggregate in generating both specificity and speed. *Philosophical Transactions of the Royal Society of London. Series B: Biological Sciences* **354**: 537–550.

Butler P, Klug A. **1971**. Assembly of the particle of tobacco mosaic virus from RNA and disks of protein. *Nature* **229**: 47–50.

Caspar D. **1964**. Assembly and stability of the tobacco mosaic virus particle. *Advances in protein chemistry* **18**: 37–121.

Citovsky V, Knorr D, Schuster G, Zambryski P. **1990**. The P30 movement protein of tobacco mosaic virus is a single-strand nucleic acid binding protein. *Cell* **60**: 637–647.

Clark JM. **1988**. Novel non-templated nucleotide addition reactions catalyzed by procaryotic and eucaryotic DNA polymerases. *Nucleic Acids Research* **16**: 9677–9686.

Dawson W, Bubrick P, Grantham G. **1988**. Modifications of the tobacco mosaic virus coat protein gene affecting replication, movement, and symptomatology. *Phytopathology* **78**: 783–789.

Deom CM, Oliver MJ, Beachy RN. **1987**. The 30-kilodalton gene product of tobacco mosaic virus potentiates virus movement. *Science* **237**: 389–394.

Destito G, Schneemann A, Manchester M. **2009**. Biomedical nanotechnology using virus-based nanoparticles. *Viruses and Nanotechnology*: 95–122.

Diaz-De-Leon F, Klotz KL, Lagrimini LM. **1993**. Nucleotide sequence of the tobacco (Nicotiana tabacum) anionic peroxidase gene. *Plant physiology* **101**: 1117.

Don R, Cox P, Wainwright B, Baker K, Mattick J. **1991**. "Touchdown"PCR to circumvent spurious priming during gene amplification. *Nucleic Acids Research* **19**: 4008.

Dujardin E, Peet C, Stubbs G, Culver JN, Mann S. **2003**. Organization of metallic nanoparticles using tobacco mosaic virus templates. *Nano Letters* **3**: 413–417.

Dunigan D, Zaitlin M. **1990**. Capping of tobacco mosaic virus RNA. Analysis of viral-coded guanylyltransferase-like activity. *Journal of Biological Chemistry* **265**: 7779–7786.

Les Erickson F, Holzberg S, Calderon-Urrea A, Handley V, Axtell M, Corr C, Baker B. **1999**. The helicase domain of the TMV replicase proteins induces the N-mediated defence response in tobacco. *The Plant Journal* **18**: 67–75.

Fang R-X, Nagy F, Sivasubramaniam S, Chua N-H. **1989**. Multiple cis regulatory elements for maximal expression of the cauliflower mosaic virus 35S promoter in transgenic plants. *The Plant Cell Online* **1**: 141–150.

Fedorkin O, Schiemann J, Baulcombe D, Atabekov J, others. **1997**. Complementation of a potato virus X mutant mediated by bombardment of plant tissues with cloned viral movement protein genes. *Journal of General Virology* **78**: 2077–2083.

Fraenkel-Conrat H, Williams RC. **1955**. Reconstitution of active tobacco mosaic virus from its inactive protein and nucleic acid components. *Proceedings of the National Academy of Sciences of the United States of America* **41**: 690.

Gallie DR, Walbot V. **1990**. RNA pseudoknot domain of tobacco mosaic virus can functionally substitute for a poly (A) tail in plant and animal cells. *Genes \& development* **4**: 1149–1157.

Gleba Y, Klimyuk V, Marillonnet S. **2007**. Viral vectors for the expression of proteins in plants. *Current Opinion in Biotechnology* **18**: 134–141.

Goelet P, Lomonossoff G, Butler P, Akam M, Gait M, Karn J. **1982**. Nucleotide sequence of tobacco mosaic virus RNA. *Proceedings of the National Academy of Sciences* **79**: 5818–5822.

Gonsalves D, Garnsey S, others. **1989**. Cross-protection techniques for control of plant virus diseases in the tropics. *Plant disease* **73**: 592–597.

Goregaoker SP, Culver JN. **2003**. Oligomerization and activity of the helicase domain of the tobacco mosaic virus 126-and 183-kilodalton replicase proteins. *Journal of virology* **77**: 3549–3556.

Grdzelishvili VZ, Chapman SN, Dawson WO, Lewandowski DJ. **2000**. Mapping of the Tobacco Mosaic Virus Movement Protein and Coat Protein Subgenomic RNA Promoters in Vivo. *Virology* **275**: 177–192.

Guilley H, Jonard G, Kukla B, Richards K. **1979**. Sequence of 1000 nucleotides at the 3′ end of tobacco mosaic virus RNA. *Nucleic acids research* **6**: 1287–1308.

Hamamoto H, Watanabe Y, Kamada H, Okada Y. **1997**. A single amino acid substitution in the virus-encoded replicase of tomato mosaic tobamovirus alters host specificity. *Molecular plant-microbe interactions* **10**: 1015–1018.

Horton RM. **1995**. PCR-mediated recombination and mutagenesis. *Molecular biotechnology* **3**: 93–99.

Ishikawa M, Meshi T, Motoyoshi F, Takamalsu N, Okada Y. **1986**. In vitro mutagenesis of the putative replicase genes of tobacco mosaic virus. *Nucleic acids research* **14**: 8291–8305.

Kamer G, Argos P. **1984**. Primary structural comparison of RNA-dependent polymerases from plant, animal and bacterial viruses. *Nucleic Acids Research* **12**: 7269–7282.

Kawakami S, Watanabe Y, Beachy RN. **2004**. Tobacco mosaic virus infection spreads cell to cell as intact replication complexes. *Proceedings of the National Academy of Sciences of the United States of America* **101**: 6291–6296.

Kegel WK, van der Schoot P. **2006**. Physical regulation of the self-assembly of tobacco mosaic virus coat protein. *Biophysical journal* **91**: 1501–1512.

Khvorova A, Lescoute A, Westhof E, Jayasena SD. **2003**. Sequence elements outside the hammerhead ribozyme catalytic core enable intracellular activity. *Nature Structural \& Molecular Biology* **10**: 708–712.

Klug A. **1999**. The tobacco mosaic virus particle: structure and assembly. *Philosophical Transactions of the Royal Society of London. Series B: Biological Sciences* **354**: 531–535.

Knapp E, Achor D, Lewandowski DJ. **2007**. Tobacco mosaic virus defective RNAs expressing C-terminal methyltransferase domain sequences are severely impaired in long-distance movement in Nicotiana benthamiana. *Virology* **367**: 82–91.

Knorr DA, Dawson WO. **1988**. A point mutation in the tobacco mosaic virus capsid protein gene induces hypersensitivity in Nicotiana sylvestris. *Proceedings of the National Academy of Sciences* **85**: 170–174.

Kobayashi M, Seki M, Tabata H, Watanabe Y, Yamashita I. **2010**. Fabrication of aligned magnetic nanoparticles using tobamoviruses. *Nano letters* **10**: 773–776.

Laemmli UK, others. **1970**. Cleavage of structural proteins during the assembly of the head of bacteriophage T4. *nature* **227**: 680–685.

Lehto K, Grantham G, Dawson W. **1990**. Insertion of sequences containing the coat protein subgenomic RNA promoter and leader in front of the tobacco mosaic virus 30K ORF delays its expression and causes defective cell-to-cell movement. *Virology* **174**: 145–157.

Lim J-S, Kim S-M, Lee S-Y, Stach EA, Culver JN, Harris MT. **2010**. Quantitative study of Au (III) and Pd (II) ion biosorption on genetically engineered tobacco mosaic virus. *Journal of colloid and interface science* **342**: 455–461.

Liu R, Vaishnav RA, Roberts AM, Friedland RP. **2013**. Humans Have Antibodies against a Plant Virus: Evidence from Tobacco Mosaic Virus. *PloS one* **8**: e60621.

López-Moya JJ, García JA. **2000**. Construction of a stable and highly infectious intron-containing cDNA clone of plum pox potyvirus and its use to infect plants by particle bombardment. *Virus research* **68**: 99–107.

Lu A-H, Salabas EL, Schüth F. **2007**. Magnetic nanoparticles: synthesis, protection, functionalization, and application. *Angewandte Chemie International Edition* **46**: 1222–1244.

Lu B, Stubbs G, Culver JN. **1998**. Coat protein interactions involved in tobacco mosaic tobamovirus cross-protection. *Virology* **248**: 188–198.

Manchester M, Singh P. **2006**. Virus-based nanoparticles (VNPs): platform technologies for diagnostic imaging. *Advanced drug delivery reviews* **58**: 1505–1522.

Mao C, Solis DJ, Reiss BD, Kottmann ST, Sweeney RY, Hayhurst A, Georgiou G, Iverson B, Belcher AM. **2004**. Virus-based toolkit for the directed synthesis of magnetic and semiconducting nanowires. *Science* **303**: 213–217.

Marillonnet S, Thoeringer C, Kandzia R, Klimyuk V, Gleba Y. **2005**. Systemic Agrobacterium tumefaciens-mediated transfection of viral replicons for efficient transient expression in plants. *Nature biotechnology* **23**: 718–723.

Más P, Beachy RN. **1999**. Replication of tobacco mosaic virus on endoplasmic reticulum and role of the cytoskeleton and virus movement protein in intracellular distribution of viral RNA. *The Journal of cell biology* **147**: 945–958.

McCormick AA, Palmer KE. **2008**. Genetically engineered Tobacco mosaic virus as nanoparticle vaccines. *Expert review of vaccines* **7**: 33–41.

McLean BG, Zupan J, Zambryski PC. **1995**. Tobacco mosaic virus movement protein associates with the cytoskeleton in tobacco cells. *The Plant Cell Online* **7**: 2101–2114.

Meric B, Kerman K, Marrazza G, Palchetti I, Mascini M, Ozsoz M. **2004**. Disposable genosensor, a new tool for the detection of NOS-terminator, a genetic element present in GMOs. *Food Control* **15**: 621–626.

Meshi T, Watanabe Y, Saito T, Sugimoto A, Maeda T, Okada Y. **1987**. Function of the 30 kd protein of tobacco mosaic virus: involvement in cell-to-cell movement and dispensability for replication. *The EMBO journal* **6**: 2557.

Namba K, Pattanayek R, Stubbs G. **1989**. Visualization of protein-nucleic acid interactions in a virus: Refined structure of intact tobacco mosaic virus at 2.9 Å resolution by X-ray fiber diffraction. *Journal of molecular biology* **208**: 307–325.

Öberg B, Philipson L. **1972**. Binding of histidine to tobacco mosaic virus RNA. *Biochemical and biophysical research communications* **48**: 927–932.

Ohno T, Aoyagi M, Yamanashi Y, Saito H, Ikawa S, Meshi T, Okada Y. **1984**. Nucleotide sequence of the tobacco mosaic virus (tomato strain) genome and comparison with the common strain genome. *Journal of biochemistry* **96**: 1915–1923.

Ohno T, Okada Y, Shimotohno K, Miura K, Shinshi H, Miwa M, Sugimura T. **1976**. Enzymatic removal of the 5′-terminal methylated blocked structure of tobacco mosaic virus RNA and its effects on infectivity and reconstitution with coat protein. *FEBS letters* **67**: 209–213.

Okada Y. **1999**. Historical overview of research on the tobacco mosaic virus genome: genome organization, infectivity and gene manipulation. *Philosophical Transactions of the Royal Society of London. Series B: Biological Sciences* **354**: 569–582.

Osman T, Buck K. **1997**. The tobacco mosaic virus RNA polymerase complex contains a plant protein related to the RNA-binding subunit of yeast eIF-3. *Journal of virology* **71**: 6075–6082.

Padgett HS, Beachy RN. **1993**. Analysis of a tobacco mosaic virus strain capable of overcoming N gene-mediated resistance. *The Plant Cell Online* **5**: 577–586.

Rae CS, Wei Khor I, Wang Q, Destito G, Gonzalez MJ, Singh P, Thomas DM, Estrada MN, Powell E, Finn M, *et al.* 2005. Systemic trafficking of plant virus nanoparticles in mice via the oral route. *Virology* **343**: 224–235.

Rietveld K, Linschooten K, Pleij CW, Bosch L. **1984**. The three-dimensional folding of the tRNA-like structure of tobacco mosaic virus RNA. A new building principle applied twice. *The EMBO journal* **3**: 2613.

Richards K, GUILLEY H, JONARD G, HIRTH L. **1978**. Nucleotide Sequence at the 5′ Extremity of Tobacco-Mosaic-Virus RNA. *European Journal of Biochemistry* **84**: 513–519.

Rogers SO, Starmer WT, Castello JD. **2004**. Recycling of pathogenic microbes through survival in ice. *Medical hypotheses* **63**: 773–777.

Rochon D, Siegel A. **1984**. Chloroplast DNA transcripts are encapsidated by tobacco mosaic virus coat protein. *Proceedings of the National Academy of Sciences* **81**: 1719–1723.

Rosypal S. **2006**. *Úvod do molekulární biologie*.

Roy G, Weisburg S, Rabindran S, Yusibov V. **2010**. A novel two-component Tobacco mosaic virus-based vector system for high-level expression of multiple therapeutic proteins including a human monoclonal antibody in plants. *Virology* **405**: 93–99.

Shew HD, Lucas GB, others. **1991**. *Compendium of tobacco diseases.* American Phytopathological Society.

Shukla S, Ablack AL, Wen AM, Lee KL, Lewis JD, Steinmetz NF. **2012**. Increased tumor homing and tissue penetration of the filamentous plant viral nanoparticle Potato virus X. *Molecular pharmaceutics* **10**: 33–42.

Siegel A. **1971**. Pseudovirions of tobacco mosaic virus. *Virology* **46**: 50–59.

Sievers F, Wilm A, Dineen D, Gibson TJ, Karplus K, Li W, Lopez R, McWilliam H, Remmert M, *et al.* 2011. Fast, scalable generation of high-quality protein multiple sequence alignments using Clustal Omega. *Molecular systems biology* **7**.

Sleat DE, Gallie DR, Watts JW, Deom CM, Turner PC, Beachy RN, Wilson TMA. **1988**. Selective recovery of foreign gene transcripts as virus-like particles in TMV-infected transgenic tobaccos. *Nucleic acids research* **16**: 3127–3140.

Smith ML, Lindbo JA, Dillard-Telm S, Brosio PM, Lasnik AB, McCormick AA, Nguyen LV, Palmer KE. **2006**. Modified Tobacco mosaic virus particles as scaffolds for display of protein antigens for vaccine applications. *Virology* **348**: 475–488.

Takamatsu N, Watanabe Y, Meshi T, Okada Y. **1990**. Mutational analysis of the pseudoknot region in the 3'noncoding region of tobacco mosaic virus RNA. *Journal of virology* **64**: 3686–3693.

Turner D, Butler P. **1986**. Essential features of the assembly origin of tobacco mosaic virus RNA as studied by directed mutagenesis. *Nucleic acids research* **14**: 9229–9242.

Turner DR, Joyce LE, Butler PJG. **1988**. The tobacco mosaic virus assembly origin RNA: functional characteristics defined by directed mutagenesis. *Journal of molecular biology* **203**: 531–547.

Turpen TH, Reinl SJ, Charoenvit Y, Hoffman SL, Fallarme V, Grill LK. **1995**. Malaria epitopes expressed on the surface of recombinant tobacco mosaic virus. *Nature Biotechnology* **13**: 53–57.

Tzfira T, Citovsky V. **2008**. *Agrobacterium: from biology to biotechnology*. Springer.

Wang H, Planchart A, Stubbs G. **1998**. Caspar carboxylates: the structural basis of tobamovirus disassembly. *Biophysical journal* **74**: 633–638.

Watanabe Y, Emori Y, Ooshika I, Meshi T, Ohno T, Okada Y. **1984**. Synthesis of TMV-specific RNAs and proteins at the early stage of infection in tobacco protoplasts: transient expression of the 30K protein and its mRNA. *Virology* **133**: 18–24.

Werner S, Marillonnet S, Hause G, Klimyuk V, Gleba Y. **2006**. Immunoabsorbent nanoparticles based on a tobamovirus displaying protein A. *Proceedings of the National Academy of Sciences* **103**: 17678–17683.

Wilson TMA. **1984**. Cotranslational disassembly of tobacco mosaic virus in vitro. *Virology* **137**: 255–265.

Wu X, Xu Z, Shaw JG. **1994**. Uncoating of tobacco mosaic virus RNA in protoplasts. *Virology* **200**: 256–262.

Yi H, Nisar S, Lee S-Y, Powers MA, Bentley WE, Payne GF, Ghodssi R, Rubloff GW, Harris MT, Culver JN. **2005**. Patterned assembly of genetically modified viral nanotemplates via nucleic acid hybridization. *Nano Letters* **5**: 1931–1936.

Zimmern D. **1975**. The 5′ end group of tobacco mosaic virus RNA is m7G5′ ppp5′ Gp. *Nucleic acids research* **2**: 1189–1202.

Zimmern D, Butler P. **1977**. The isolation of tobacco mosaic virus RNA fragments containing the origin for viral assembly. *Cell* **11**: 455–462.